Response to Editor David Ham:

We highly appreciate your positive reminders and suggestions to ensure that the experimental dataset, analysis scripts for the results and the model code can meet GMD's requirements for publishing article. Our detailed responses (**Bold**) to each question are listed below.

(1) No model source code. The code and data availability section merely states that code is not available due to "the confidentiality requirement". GMD does permit model code to be withheld from publication if this is unavoidable for reasons beyond the control of the authors. Usually this is because the copyright licence of the code does not permit redistribution. However, the reasons that the authors cannot release the code must be detailed in the code and data availability section. In particular, it is important to state who can get a licence and how.

We agree with the reviewer and appreciate this helpful suggestion. We have added the reason that we cannot release the code in the "code and data availability" part, which is "the model code cannot be distributed due to the copyright licence requirement from the Numerical Weather Prediction Center of China Meteorological Administration (NWPC/CMA). If someone wants to use the GRAPES_GFS model or reproduce these experiments in this article, he/she can contact the operational management department of NWPC/CMA via email songzx@cma.gov.cn or phone +86-10-68400477."

(2) Version not identified. Neither the title of the manuscript nor the code and data availability section state precisely which version of GRAPES_GFS was used. This makes it impossible to reproduce the work even if one has a licence.

Sorry for our mistake. We adopted the version 2.3.1 of GRAPES_GFS in this research and now have specified it in the manuscript:

1) Lines 17 and 18: "Then, the characteristics of spin-ups in the version 2.3.1 of GRAPES (Global/Regional Assimilation and Prediction System) global forecast system (GRAPES_GFS2.3.1) under different initial fields are compared and analyzed."

2) Line 127: "On 1 July 2018, the GRAPES global 4-dimensional variational (4D-Var) data assimilation system has been in operation (Zhang et al., 2019), which is called version 2.3.1 of GRAPES_GFS (abbreviated as GRAPES_GFS_2.3.1). And the GRAPES_GFS_2.3.1 version was adopted in this research."

3) We also specified the model version in the rest of the manuscript.

(3)Model data is not on a persistent public repository. The model data appears to be on a cloud storage provided by Baidu. This lacks the persistence, non-revocability and persistent identifiers required for a journal publication. The data should instead be stored in a properly persistent archive with a persistent identifier such as a DOI. I note in this regard that the authors are from national laboratories so I would expect such facilities to be available to them.

The reviewer proposed a good question. However, our lab doesn't provide a data-sharing platform for individuals, so I had to buy cloud storage of Baidu to share these dataset. I have purchased five years of service and will be able to renew my account in the future. Meanwhile, I stored the data in our high-performance computer storage devices. These could guarantee long-term sharing of the experimental data.

(4) No configuration, run, or data processing scripts. The configuration files, run scripts and any data processing or analysis scripts used to produce the results presented in the manuscript need to be publicly and persistently archived, and cited from the code and data availability section. As a guide, every file the user would need to reproduce the manuscript should accessible.

The experimental configuration file and the data processing and analysis scripts used to produce the results presented in the manuscript have been uploaded to the website.
1) The directory of "*data_processing_scripts*" includes all the analysis scripts for plotting the results.
2) The directory of "*model_configure*" includes the configure files and run scripts for the GRAPE_GFS.

Response to Reviewer 1:

We thank the anonymous referee for his/her valuable comments and suggestions that have helped us improve the paper quality. Our detailed responses (**Bold**) to the reviewer's questions and comments (*Italic*) are listed below.

Anonymous Referee #1:

Overview:

This paper examines the impact of initial conditions on the spin-up process in the GRAPES_GFS model, with results showing that the external FNL analysis is inferior to the model's internal analysis and that the removal of hydrometeor information during the cycling process has a deleterious effect and necessitates further spin-up time. These conclusions are convincingly examined from numerous angles, although the findings are somewhat as expected. Because of that, the paper would benefit from a bit more explanation of the motivation of the work (e.g., did the FNL used to be used prior to the 4DVAR upgrade? Why is it that the hydrometeor data is wiped out during the cycling process, and is changing that currently under consideration?). There are also a few spots in the analysis, particularly of the tendencies, where there appear to be a few errors in labeling/incongruencies with the cited figures or sections that are unclear. A few of the figures could also stand to be a bit clearer in their labeling and font size. Finally, while the paper's writing is fairly good, there remain widespread instances of misused articles and awkward words and phrases that sometimes obscure the clarity of what is trying to be conveyed, some of which are noted in the technical corrections below. That said, the motivation of the work is sound and the analysis appears to be solid, so pending the specific comments listed below I believe the manuscript should be published.

We highly appreciate the reviewer's positive evaluation about this study. We also thank the reviewer for the valuable and detailed comments and suggestions which have helped us improve the paper quality.

For the suggestion in the overview, we added/revised two more detailed explanations in corresponding section (Line 89 and Lines 95 - 102, respectively) to clarify the motivation of this study.

(1) For the suggestion that "(e.g., did the FNL used to be used prior to the 4DVAR upgrade?)".

No, FNL data was not used as initial field in the GRAPES_GFS operation. However, it used to be used in the model research and development. For the GRAPES-GFS batch experiment, the cold-start simulation tends to consume less computing resources than cycle assimilation simulation, and the developers can faster obtain their wanted results. Therefore, in the development/modification of GRAPES_GFS, FNL data as the model's initial field is usually first adopted to simulate and evaluate the impact of modification in the dynamic core and physical process on forecast performance. When the result is ideal, then the cycle experiment with 3D-VAR/4D-VAR is carried out and its forecast

output is used to analyze the final effect of the modification.

We added the following sentence in Line 91 to describe how the FNL data is used in research and development of the GRAPES-GFS.
"In the research and development of the GRAPES-GFS, the widely-used FNL (Final Operational Global Analysis) reanalysis data provided by NCEP (National Centers for Environmental Prediction) (Kalnay et al., 1996) is usually adopted as the model's initial field to quickly evaluate the effects of modification in dynamic core and physical processes on the model forecast performance, because the cold start simulation with FNL consumes less computing resources than that of cycle assimilation simulation. What advantages does the new 4D-VAR assimilation analysis fields have in spin-up process compared with the cold start simulation with FNL?"

(2) For the question "Why is it that the hydrometeor data is wiped out during the cycling process, and is changing that currently under consideration?" we gave a detailed reply (as reply to comment 3) and revised the corresponding section in Lines 95 - 102.

Specific Comments:

Line 25: Changing "variation amplitudes" to "variations in amplitude…" may be clearer here.
We agree with the reviewer and changed Line 25 to "…, because the variations in amplitude of the temperature and humidity tendency..."

Lines 81, 144: By "resolution", do the authors actually mean the "grid spacing"?
Yes, the "resolution" in Lines 81 and 144 means "grid spacing", which is more specific and accurate. We changed "resolution" to "grid spacing" in the corresponding lines.

Lines 95-102: If I am understanding correctly, the operational model includes 3 hours of "built in" spin-up time so that forecasters looking at a launched forecast don't have to discard the first few hours of the model run. If that is the case, why is it that the hydrometeor variables are discarded? Is it due to limitations of disk space during the restart? Because this seems like something that would predictably introduce problems and negate the benefits of spinning the model up earlier (which the results of the paper confirm), I think it would be helpful for the authors to provide a bit of history about why this is currently done.
It is a good suggestion. We agree with the reviewer and it would be helpful to improve the understanding for the motivation/background of the study when we give a further introduction why the cloud-field variables are discarded and provide the reasons why this is currently done.
For users (especially forecasters) of numerical weather prediction models, they are usually accustomed to using the forecast productions of numerical models staring to integrate from 00 UTC or 12 UTC (or more time, 06 UTC, 18 UTC). We adjusted the operational process of GRAPES_GFS to adapt to user's usage habit. We take 00 UTC as

an example for explanation. GRAPES_GFS uses the 4D-Var assimilation system to improve the initial field quality. For 00 UTC, 4D-var assimilation system needs to perform data assimilation analysis using the model meteorological fields of the first three hours (21 UTC), and finally generate assimilation analysis field at 21 UTC, that is, the initial field of the G21 experiment. Considering the user's habits, the model at 00 UTC is terminated after three hours integration from 21 UTC. In the process, only the essential meteorological field variables (u, v, th, qv, pi, ps, etc.) are retained for restart, while the existing cloud-field variables (the mass and concentration of hydrometeors and cloud cover) are discarded. The model restarts using the above retained variables at 00 UTC, and its forecast products are used to release to users, which is the G00 experiment.
The reasons for the unretained cloud field variables are mainly based on the following considerations: the hydrometeor contents are very small amount relative to water vapor and they can be quickly created in the spin-up process when the model restarts. Moreover, it can save storage space and IO time. However, there are no studies that have carefully analyzed and evaluated its impact on the spin-up process and model forecasts. This is the focus of this paper.

We revised the content in Lines 95 - 102 to more clearly describe the changes of model forecast variables during the terminated-restart process of GRAPES-GFS and the reasons why the impact of the loss of cloud-field variables can be accepted in operation.
"Actually, for numerical weather prediction model's users (especially forecasters), they are usually accustomed to referring the forecast productions of numerical models staring to integrate from 00 UTC or 12 UTC (or more time, 06 UTC, 18 UTC). Thus, considering the habit of users in using the forecast results, GRAPES_GFS integrates for 3 hours (to 1200 UTC) to retain the essential meteorological element fields (U, V, T, Q, H, TS , Ps, etc.), and then the integration is terminated and restarts from 1200 UTC by using the new-saved meteorological field data. The model forecast results thereafter are released, that is, the forecast results at 1200 UTC are obtained by users. In this process, the cloud-field variables (the mass and concentration of hydrometeors and cloud cover) during the first 3 hours of integration are not retained in the model, losing the cloud information formed after the 3-hour spin-up. The reasons for the unretained cloud-field variables were mainly based on the following considerations: the hydrometeor contents are very small amount relative to water vapor and they can be quickly created in the spin-up process when the model restarts. Moreover, this treatment can save storage space and input/output (IO) time. However, its impacts on the spin-up process and the model forecast performance have not yet been carefully analyzed and evaluated."

Line 129: Consider removing "weather process" here, as I think the sentence reads more clearly without it.
We agree with the reviewer and removed "weather process in" in Line 129.

Lines 134-135: The sentence beginning "In the second experiment" is quite unclear to me. What "results" are being talked about here? How is an "initial field" used? The following sentence is clearer in terms of what is actually being done, so consider rephrasing or

removing.

We agree with the reviewer that the description for the second experiment is not too clear. Here, the "results" means the forecast output from the second experiment, and we originally wanted to express: the model output of the second experiment is exactly the forecast results to be provided to users by GRAPES_GFS in operation. The "initial field" of the second experiment has been explained in the rephrased section. According to the reviewer's suggestion, we rephrased the description for the second experiment as follows:

"For the second experiment, called G00, its initial field adopts 3 hours integration output of G21 without retaining cloud-field information. That is to say, at 0000 UTC on August 9, it retains the G21's 3-h forecast variables (u and v wind field components, potential temperature, water vapor and dimensionless air pressure, etc.) required by the pre-processing system and stops the integration. During the process, the fields of all hydrometeor contents and cloud cover are lost considering the limitation of IO time and disk space. And then the model restarts at 0000 UTC on August 9 with the reserved forecast-field information for forecasting in G00. Moreover, the model output of G00 is exactly the forecast results to be provided to users in the GRAPES_GFS operation."

Line 187: What is meant by the "co-action of cloud and convections" here? Is this co-action shown in the figure?

It is a good suggestion, and we provide further explanation in the section. In the GRAPES_GFS, the variation of water vapor is determined by dynamic core (DYN), turbulent mixing of planetary boundary layer (PBL), cumulus convection process (CONV) and cloud physical process (CLOUD). Among them, the sum of the last three items is referred to as the total tendency of all physical processes (PHY). In Figs. 2b and 2e, we can see that the variations of WVTs from DYN and PBL are much smaller compared with CONV and CLOUD, thus we originally descripted it in this section "…, while the variation of water vapor is mainly caused by the co-action of cloud and convections". To describe this part more clearly, we rephrased it as follows.

"At these levels in G21 (Figs. 2b and 2e), the total WVTs at the first few integration steps are slightly larger than that at the subsequent integration steps. The variations of the WVTs from dynamic core and turbulent mixing process in the planetary boundary layer are much less than those from the cumulus convection process and cloud physical process, and the latter two processes jointly determined the variation of WVTs at 300 hPa and 500 hPa."

Lines 195-196 and elsewhere: Does "physical process" here refer to the line labeled PHY in Fig. 2, or all 'physical processes' in the model (versus dynamic)? Make sure this is clear throughout the text. The text also states that the biggest difference between F00 and G21 is caused by the convection scheme, but it appears to me that the PHY line is also significantly different between the two.

We agree with the reviewer's comment and it is a good suggestion. Yes, the "physical process" throughout the text refers to "all physical processes" (versus dynamic core) in the GRAPES_GFS. We checked throughout the text and changed the "physical process"

to "all physical processes" in order to clarify its exact meaning, which means the total tendency of all physical processes in the model.

Since PHY represents the total water vapor tendency of all physical processes, it includes the contribution of the convection scheme, thus the PHY lines between F00 and G21 also takes roles on significant difference. Their difference of WVT between the two experiments is essentially caused by convection scheme (Figure 2g and 2h).

In addition, at the beginning of section 3.1.2, we added the following description to state the compositions of tendency of temperature and water vapor in the GRAPES_GFS, which can benefit to a better understanding.

"In the GRAPES_GFS, the total temperature tendency of the model (ALL) is determined by dynamic core (DYN), radiation process (RAD), turbulent mixing in planetary boundary layer process (PBL), cumulus convection process (CONV) and cloud physical process (CLOUD). Among them, the total temperature tendency of all physical processes (PHY) is defined as the sum of the last four items (PHY=RAD+PBL+CONV+CLOUD). Likewise, the total water vapor tendency for ALL and PHY are same to those of temperature tendency except for the radiation process (RAD). "

Section 3.1.2 overall: Related to the previous comment, it would be helpful if the authors state more explicitly how each of the tendencies in Figs 2, 3, etc are defined. 'RAD' and 'PBL' are somewhat straightforward, but the authors should state clearly where the CLOUD, CONV, and PHY tendencies are coming from and how they all differ.
We agree with the reviewer. Except for the reply to the previous comment, we added corresponding description for all abbreviations (ALL, PHY, RAD, PBL, CONV and CLOUD) in Figs 2, 3 to state them clearly. The modifications for Figs 2 and Figs 3 are as below:

"Figure 2. Time evolution of mean water vapor tendency (WVT) of dynamical core (DYN), planetary boundary layer process (PBL), cumulus convection process (CONV), cloud physical process (CLOUD), the total of all physical processes (PHY, PHY=PBL+CONV+CLOUD) and the total of the model (ALL, ALL=DYN+PHY) at 300hPa, 500hPa and 925hPa heights from 0 to 1h simulated by F00 (a,d,g), G21(b,e,h) and G00(c,f,i) experiments. Unit: g/kg/day."

"Figure 3. Time evolution of mean temperature tendency (TT) of dynamical core (DYN), radiation process (RAD), planetary boundary layer process (PBL), cumulus convection process (CONV), cloud physical process (CLOUD), the total of all physical processes (PHY, PHY=RAD+PBL+CONV+CLOUD) and the total of the model (ALL, ALL=DYN+PHY) at 300hPa, 500hPa and 925hPa heights from 0 to 1h simulated by F00 (a,d,g), G21(b,e,h) and G00(c,f,i) experiments. Unit: K/day."

Line 211: Please add reference to Figure 3 here.

We added the figure reference in line 211.

"In the middle and upper layers of the model, the dramatic change of the TT in F00 mainly occurs within the first half hour of the integration (Figs. 3a and 3d)."

Line 212: Again, related to comments 7 and 8, the authors state that it is due to "Cloud and convection processes", but Fig. 2a,d seems to show the biggest changes due to CLOUD and PHY rather than CONV (black line). Please clarify.

We agree with the reviewer. It can easily cause errors in understanding if we do not clarify the meaning of CLOUD, CONV and PHY in Figure 2 and Figure 3. We modified the descriptions for Figures 2, 3 in the reply to comments 7 and 8. Because the temperature tendency (TT) of PHY in Figure 3 is the total TT related with physical processes, PHY=RAD+PBL+CONV+CLOUD, it is reasonable that the TT of PHY shows changes consistent with that of CLOUD that is biggest variation in amplitude among the physical processes shown in Figure 2a,2d and Figure 3a,3d.

For the changes of water vapor tendency (WVTs, Figure 2a,2d) and temperature tendency (TTs, Figure 3a,3d) in the F00 experiment, although the directions of their change conform to the physical laws (condensation process leads to negative water vapor tendency and positive temperature tendency, vice versa), their variations in amplitude are quite different. The variation in amplitude of TTs appears to be more dramatic than that of WVTs. Among all the TTs shown in Figure 3a and 3d, the cloud physical process is the biggest one in the first time step, followed by convection process. The TT and WVT of convection process decrease rapidly after one time step. Based on the above description, the original expression in line 212 is not appropriate and we modified it as follows:

"Among all the TTs at the first integration step, the cloud physical process leads to the biggest one, followed by convection process, and they are related with the water vapor condensation process (Figs. 2a and 2d)."

At the same time, we deleted the following sentence "Compared with the convection process, the cloud physical process can cause greater temperature adjustments." to keep the meaning coherent in this section.

Line 222: It appears to me that the DYN and particularly the PHY line in Fig. 3g show much smaller adjustments than the middle and upper levels, not larger. Please clarify.

Sorry for our mistake and thanks for helping figure it out. We corrected "a relatively large and rapid adjustment" to "a relatively small and rapid adjustment" in Line 222.

Line 223: Re: "dehumidifying and heating of the atmosphere", doesn't Fig. 3g show an overall cooling of the atmosphere (negative TT for the ALL line), corresponding to a generally positive overall WVT in 2g?

In line 223, we had wanted to describe the temperature tendency (TT) of the convection scheme first since it is different from other physical processes and dynamic core. We rephrased this section as follows:

"The TT of the convection process at 925 hPa in F00 varies between 1.5 K d^{-1} and 2 K d^{-1}, which is mainly caused by condensing and dehumidifying of the atmosphere (Fig. 2g). Except for the cloud physical process with a relatively small positive tendency in the first four time steps, the TTs of dynamic core and other physical processes are all negative. Overall, in F00 the total atmospheric temperature is reduced with an amplitude of about -1.2 K d^{-1} in the first hour of the integration at 925 hPa."

Line 237: It appears to me that the adjustments in G00 are almost half those in G21 at all levels (at least for the first few integrations) and not what I would characterize as "close to or slightly smaller".

We believe that the reviewer's description for the difference of TT between G00 and G21 in Line 237 is more accurate and we modified the sentence as follows:

"In the first few time steps, G00 also has an adjustment process, with the adjustment amplitudes of TT close to half those in G21 at all levels."

Line 248: Please define how the total hydrometeor content is defined (even if it is just cloud + ice + rain + snow + hail, etc.).

We agree with the reviewer and added the definition for the total hydrometeor content in the sentence of Line 248, "The total hydrometeors content (THC, THC = cloud water + raindrop + cloud ice + snow + graupel) greater than…"

Lines 258-259: Is that how the equilibrium state is being defined overall, or is the description given here (24 hours vs. 6 hours below 850 hPa) only for this case? It seems more accurate to state that the equilibrium state is defined as when the difference with respect to the 24-hour integration is minimal, implicitly assuming that equilibrium will have been reached by 24 hours. Also, please quantify what "is insignificant" means here. Is it just being used subjectively?

It is a good comment on the description for the definition of equilibrium state. We wanted to give an introduction of the equilibrium state for levels below 850 hPa in lines 258-259. Certainly, it would be more conducive to the quantitative analysis of spin-up time if the definition of equilibrium state applicable to all levels is given. In fact, it is difficult to quantitatively determine the time to complete spin-up process in model because of the comprehensive adjustment and changes from the dynamic and the physical processes. We have drawn the distribution of total grid number of cloud (TGNC) of 48-h and 72-h, and we found their vertical distributions are very close to that of 24-h. Therefore, we adopt 24-h TGNC as the reference standard to analyze the equilibrium time, which is what you mentioned "implicitly assuming that equilibrium will have been reached by 24 hours". We agree that the definition of equilibrium state you gave is more accurate and can be applicable to all levels. In our original definition, the time (after 6 hours) should not be a specific time that is used to compare with the TGNC at 24 hours. Based on the above analysis, we modified the definition of equilibrium state as follows:

"Note that the statistical equilibrium state is defined when the difference of TGNC with respect to the 24-hour integration is insignificant (the difference is less than 20% of

TGNC at 24-hour).”

We rechecked our descriptions in the section and think it is reasonable to consider 20% as insignificant difference in TGNC, which is consistent with the description for the spin-up time at all levels, while it seems a little subjective.

Lines 251-267: Can the authors add some discussion of the equilibrium “overshoot” in F00 at upper levels? This was one of the more noteworthy things I noticed about this figure.

Yes, we can and it is a good suggestion. As shown in the Fig.4a, the total grid number of cloud (TGNC) of the F00 at upper levels has a larger value than those of G00 and G21, which is mainly caused by the differences of humidity field in their initial fields. We take F00 and G21 as examples and added two additional figures (shown below) to state it. Compared with G21, F00 has a wetter water vapor environment at the upper levels (Fig.6d), which tends the water vapor to quickly condense into more hydrometeors at the beginning of the integration to eliminate supersaturated water vapor. When the model began to integrate the F00 experiment has a higher hydrometeor content value and a wider distribution of cloud region (Fig. R1 and Figs.5a and 5e), thus its TGNCs are also larger than those of G21 (Fig.4a) at the upper layers. For the cloud formation at the beginning of integration (0 to 3 timesteps), it is mainly completed through the condensation process in the cloud scheme, yet convection scheme has less contribution because it need take a certain time to reach the triggering condition and detrainment of the hydrometeors (Figs. R2a and R2b, Figs. R2a and R2d). With the integration of the model and the potential impact of advection process of dynamics on environmental humidity field, the clouds scheme is no longer dominated by the condensation process, but presents the coexistence of condensation and evaporation (Fig. R2c).

Based on the above analysis, we added the following discussion in Line 267：“Compared with G21, F00 has a wetter water vapor environment at the upper levels (Fig.6d), which tends the water vapor to quickly condense into more hydrometeors through cloud scheme to eliminate supersaturated water vapor at the beginning of the integration (Fig.2a). Thus F00 has a higher hydrometeor content value and a wider distribution of cloud region (Figs.5a and 5e) and its TGNCs are also larger than those of G21 at the upper layers.”

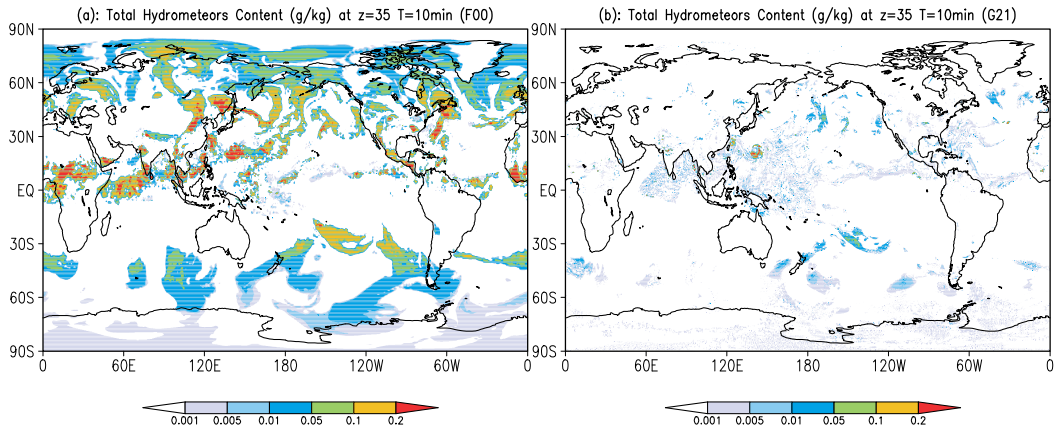

Figure R1. The total hydrometeors content of z=35 (~300hPa) at T=10min, unit: g/kg, (a) F00 experiment, (b) G21 experiment.

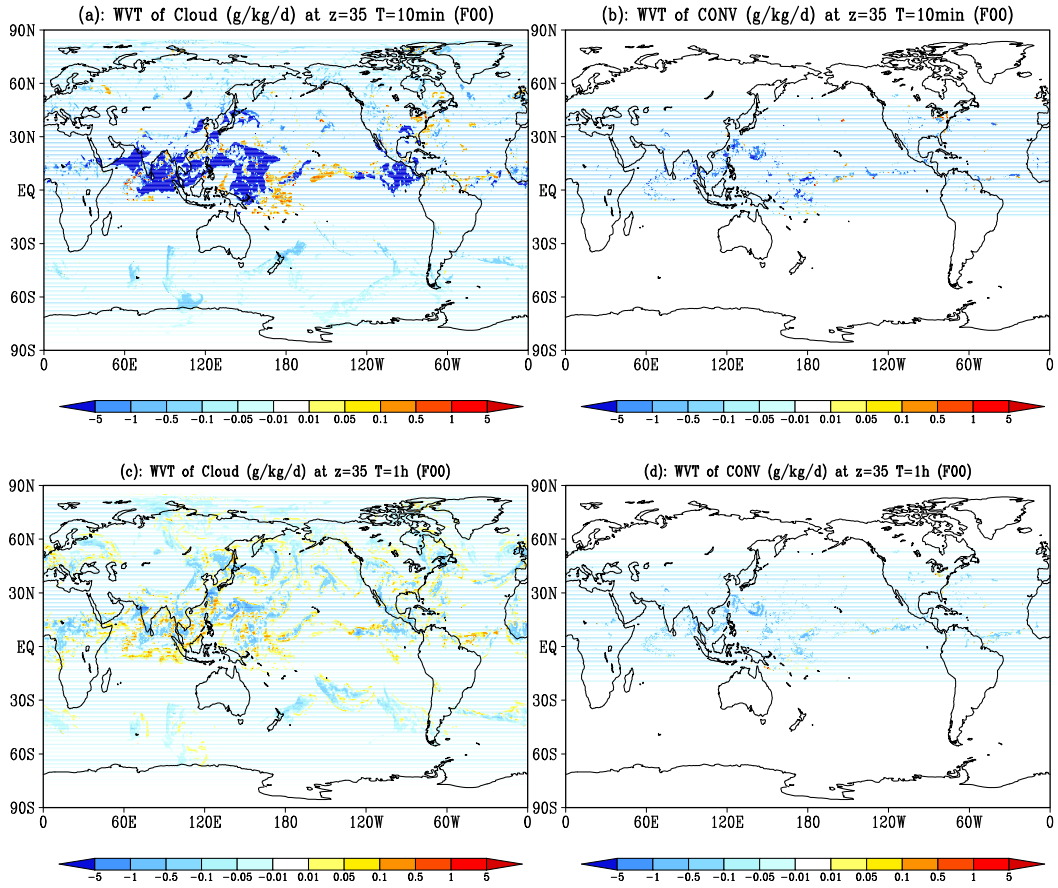

Figure R2. The water vapor tendency (WVT) at the 35 th model level (~300hPa) from (a,c) cloud scheme and (b,d) convection scheme at integrated time (a,b) 10min and (c,d) 1 hour, in F00 experiment, unit: g/kg/d.

Line 292: Should "initial time" really be 21Z (i.e., in G21)?

Yes, it is 21Z. We added this information, and added "in G21" for "that" to specify the experiment.

The sentence in line 292 was modified to: "…the atmosphere of G00 with much weaker supersaturation at initial time than that in G21."

Lines 308-309: These findings are definitely in agreement with past studies about the importance of an accurate initial moisture field, at least on the storm-scale. It may benefit the paper and further emphasize the authors' point to add some references to other papers discussing the importance of accurate moisture DA, e.g.:

Weygandt, S. S., A. Shapiro, and K. K. Droegemeier, 2002: Retrieval of model initial fields from single-Doppler observations of a supercell thunderstorm. Part II: Thermodynamic retrieval and nu- merical prediction

Ge, G., J. Gao, and M. Xue, 2013: Impacts of assimilating measurements of different state variables with a simulated supercell storm and three-dimensional variational method.

Many thanks for the information and we highly appreciate it. We added the following sentence to emphasize our point:

"It also suggests that we need to pay more attention to the analysis quality of water

vapor in data assimilation (DA). And this has been also confirmed in previous studies (Weygandt et al. 2002; Ge et al. 2013) that the accurate moisture initial field by DA is an effective way to improve the forecast performance of supercell storm in numerical weather prediction models."
Meanwhile, we added corresponding paper information in reference part.

Line 329: Do the authors mean the G21 run instead of observations? If not, what observations are being referenced here?
It is a good question. Yes, we compared the difference of forecast variables in G21 and G00 in section 3.2.1, but did not compare them with the observational dataset. In this part, we mainly focus on the differences caused by not retaining the cloud field information in G00 and we want to check if there is a systematic impact on GRAPES-GFS. When compared with the observational data, the difference changes involve many factors (dynamical core, physical processes, DA, even the model's inherent factor), which are beyond the content of this article. In the further, we will adopt more cycle experiment results to comprehensively evaluate its impact on the forecast bias.

Line 352: This sentence is unclear to me as I don't understand what is meant by "same forecasts", although I assume the authors are stating that the conclusions for both Lekima and Krosa are the same and therefore only Lekima will be presented. Please clarify.
Sorry for the confusion. The understanding of the reviewer is exactly what we would like to deliver. We modified the sentence by following the reviewer's suggestion:
"Since the conclusions for both "Lekima" and "Krosa" are the same, only "Lekima" will be presented in this study."

Line 355: Can "CCWV" and "TCIW" be made consistent with the axis labels in Fig. 9, of vice versa?
Yes, we corrected the inconsistencies of "CCWC" and "TCIW" between the text in line 355 and the axis labels in Fig. 9. Meantime, we changed "total content of ice water (TCIW)" to "column cloud ice content (CCIC)" throughout the text, which is consistent with the expression of column cloud water content (CCWC).

Figures 1, 2, 3: Tick labels are small and hard to read. Please enlarge.
We replotted Figures 1, 2, 3 and enlarged the tick labels.

Figure 4: Legend text is too small to read.
We replotted Figure 4 and enlarged the legend text.

Figures 1, 2, 3, 4: Please add titles to each subplot of what run, height, time, etc. are being shown in each panel. It is confusing having Figure 1 vary by run in each row, Figure 2 vary by run in each column, etc.
We replotted Figures 1, 2, 3, 4 according to the reviewer's suggestions. For Figure 1, we think it vary by run in each row.

Figure 7a: Are the legend labels switched here? As per the discussion, shouldn't g21_cwp be higher than g00_cwp?

Yes，the legend labels were switched in Fig. 7a. We made the correction.

Technical Corrections:

Line 32, 37, elsewhere: Change "Besides" to "In addition"
Line 43: Change "reasonability" to "representativeness"
Line 53: "model"→"modeling"
Line 56: "could" → "can"
Line 91: "widely-used" → "widely used"
Line 115: "difference" → "differencing"
Line 128: Should "1.2" be "2.2" here?
Line 143: "outputted" → "output"
Line 145: "operational solution" → "the operational setup"
Line 182: "in the" → "due to"
Lines 185-186: "this level" → "these levels"
Line 187, 198, 202, 208, elsewhere: "convections" → "convection"
Line 244: Remove "analysis"
Line 251: "no matter the" → "regardless of whether the"
Line 273: "lead time" → "forecast time"
Line 277: "at time 1 hour after" → "at 1 hour into"
Line 302: "can reflect" → "reflects"
Line 303: Remove "relatively"
Line 305: "It" → "This"
Line 312: "in the operation" → "operationally"
Line 313: "less THC" → "decreased THC"
Line314: Remove "situation"
Line 315, 351: "typhoon track" → "track"; "landed on" → "made landfall in"
Line 327: "cloud" → "clouds"
Line 334: "moments" → "times"
Line 335: "two" → "four"
Line 351: "continued to develop on ocean" → "remained offshore"; remove "from offshore areas"
Line 360: "strengthening" → "increase"
Line 368: "get" → "gets"; remove "of them"
Line 371: "an alternation of" → "alternating"
Line 374, 381: "While" → "In contrast,"
Line 382: Should "G20" here by "G21"?
Line 388: Should "Lichma" by Lekima?
Line 398: "All the three different experiments" → "All three experiments"
Line 407: "unobvious" → "not obvious"
Line 418: "analysis" → "analysis of"

We highly appreciate the detailed comments from the reviewer, and agree with the

reviewer for all the technical corrections. Based on these comments, we made corresponding changes, which have helped us improve the article's clarity. We give special responses to the questions for Lines 128, 382, and 388.

(1) Yes, "1.2" should be "2.2" in line 128.

(2) Yes, "G20" should be "G00" in line 382.

(3) Yes, "Lichma" should "Lekima" in line 388.

Response to Reviewer 2:

We thank the anonymous referee for his/her valuable comments and suggestions that have helped us improve the paper quality. Our detailed responses (**Bold**) to the reviewer's questions and comments (*Italic*) are listed below.

Anonymous Referee #2:

Overview:

The manuscript investigates the influence of spin-up and restart in a global weather forecast system GRAPES. Such a topic is important, as careful handling of those technical issues can greatly improve the accuracy of weather prediction. By comparing different spin-up and restart methods, the authors gain important knowledge of the forecasting system, such as that the GRAPES with its own analysis field performs better than the one using NCAR final reanalysis (FNL) data for the cold start in the spin-up. The paper contains useful information for model development and usage. I recommend its publication with GMD, pending on some minor comments below.

We highly appreciate the reviewer's positive evaluation about this study. We also thank the reviewer for the valuable and detailed comments and suggestions which have helped us improve the paper quality.

About the experiment setup. To better illustrate the differences between three experiments, which are of great importance to this paper, can the authors use a schematic plot to show how the three runs were performed and what are the key input data. Also, it should be explicitly stated in the Section 1.2, why those three experiments were conducted, or in other words, what we expect to learn by comparing them. The three-hour lag confuses me a little bit.

Fig. R1 shows the 4D-Var cycle assimilation system and the experiment setup. In fact, we have listed the experimental settings in Table 1. Since the contents of hydrometeor are not analyzed and updated in the 4D-Var system and the cloud information simulated by the G21 experiment is not retained during the restart in the G00 experiment, the input variables of the three tests are the same, we no longer specified the input variables for the three experiments.

To more clearly state why three experiments were conducted in the current GRAPES_GFS operational system, we rearranged the fourth paragraph in the Introduction section and added the following sentences: "Then another question is what advantages the new 4D-VAR assimilation analysis fields have in spin-up process compared with the cold start simulation with FNL.", "Actually, for numerical weather prediction model's users (especially forecasters), they are usually accustomed to referring the forecast productions of model staring to integrate from 00 UTC or 12 UTC (or more time, for example 06 UTC, 18 UTC). " , and "The reasons for the unretained cloud-field variables were mainly based on the following considerations: the hydrometeor contents are very small amount relative to water vapor and they can be quickly created in the spin-up process when the model restarts. Moreover, this treatment can save storage space and input/output (IO) time. However, its impacts on the spin-up process and model forecast performance have not yet been carefully

analyzed and evaluated. Therefore, we need to fully diagnose and analyze the necessity of the repetition of GRAPES_GFS spin-up during the re-integration, and the impact of the lost cloud-field information on the later forecast. ".

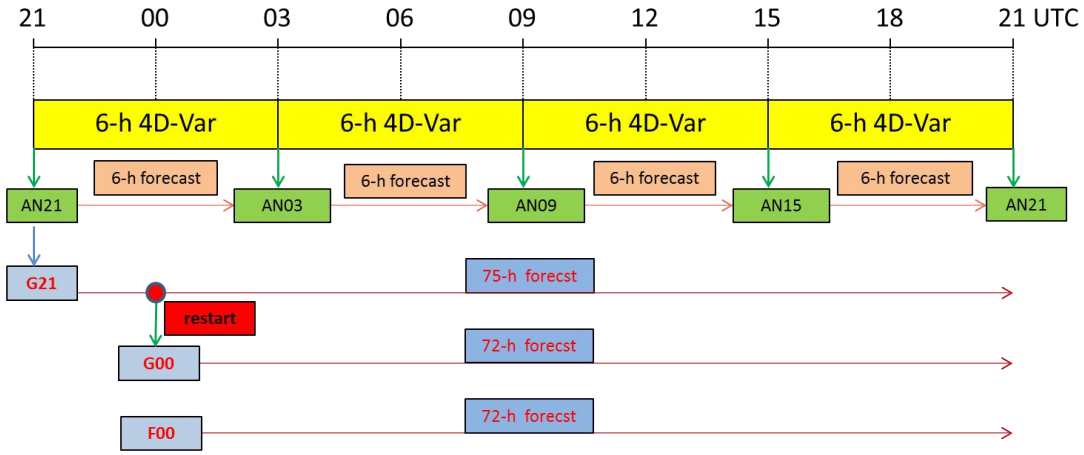

Figure R1. The schematic diagram of 4D-Var cycle assimilation system and experiment setup in this paper.

It is unclear to me what is the current protocol for spin-up and restart strategies used by CMA that uses GRAPES_GFS to conduct the daily weather prediction as well as the extreme weather prediction like typhoons. According to this study, is there any modification needed on the protocol?

It's a good question. In current protocol of operational GRAPES_GFS it still adopts analysis fields from the 4D-Var system as the model's initial field at 09UTC/21UTC and then restarts after 3hr-integration without the information of cloud fields, that is to say, same to the G21 experiment in this paper. Our research results show that it could lead to systematic biases for height, temperature and precipitation fields as well as typhoon track if the restart of the model does not include the information of cloud fields. We have told the results to the managers of NWPC/CMA, which attracted their considerable attentions. As we all know, the adjustment of numerical weather predication protocol has strict specifications, which needs to carry out parallel experiments for a period of time and evaluate the results before its operation application. The parallel experiment has been listed in the operational testing plan. If there are further results, we will be willing to share with you.

Is the total grid number of cloud (TGNC) related with the total cloud fraction? The latter is a more common term. Also, 1.0 e-4 g kg-1 threshold of cloud sounds an arbitrary choice. Are the results sensitive to this threshold definition?

It's a good question. TGNC is related with the total content of all hydrometeors (THC, that is to say, THC=cloud water + raindrop + cloud ice + snow + graupel). We define the grid with cloud when its THC is greater than 1.0 e-4 g kg-1 according to our results. We have tried three thresholds (THC= 1.0 e-5, 1.0 e-4, and 1.0 e-3, respectively) to compare the spinup time, and the results we got are basically the same. In other words, teh results seem not very sensitive to the threshold definition. Meantime, to

clarify this part more clearly, we added the description for the definition of equilibrium in section 3.1.3 as follows "Note that the statistical equilibrium state is defined when the difference of TGNC with respect to the 24-hour integration is insignificant (the difference is less than 20% of TGNC at 24-hour). " combing with the comments of the first reviewer.

Fig. 11a, why g00 and g21 are identical before 42 Hour and then become different abruptly?

The forecasted track errors before 42 Hour simulated by G00 and G21 experiments are not identical. Actually, their tracks are very close before 42 Hour, which are shown in Fig. R2. For the abrupt track difference after 42 Hour, it was caused by the continuous accumulation of the direct cloud-radiation processes, temperature difference, and even re-undergone spin-up process in the typhoon cloud area and their transmissions to the typhoon eye through dynamic processes with the integration. As stated in this paper, the restarted model (G00 experiment) with lost cloud-field information in initial field needs to re-undergo a spin-up process and causes systemic biases of cloud, temperature and geopotential height and precipitation fields at the model early forecast. These biases mainly exist in areas with clouds. For a typhoon, the differences of temperature and geopotential height of the G00 experiment initially exist in the cloud belt around the typhoon eye compared with G21 experiment. With the model integration, the peripheral system difference gradually affects the typhoon center (track) through the dynamic process. These changes can be confirmed from Fig. R3 and Fig. R4. For example, the large value area of temperature difference between G00 and G21 experiments at the early stage of integration is mainly located in the spiral cloud belt around the typhoon eye and its value can reach 2k, while its value over the typhoon central is only -0.25~0.25K. With the integration of the model, the temperature difference of the typhoon eye gradually becomes larger, and its value reaches 0.5-1K at 50 hours of integration, which is bound to affect the track of the typhoon by dynamic process.

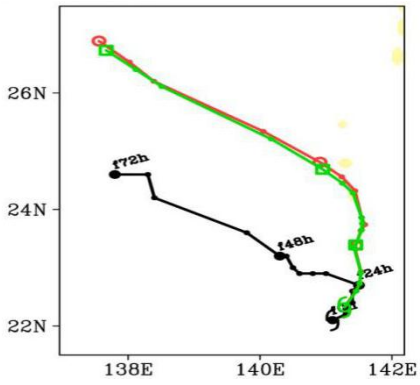

Figure R2. The track of typhoon "KROSA" observed (the black line) and simulated by G21 experiment (the green line) and G00 (the red line) experiment from 0000 UTC on August 9 to 0000 UTC on August 12, 2019.

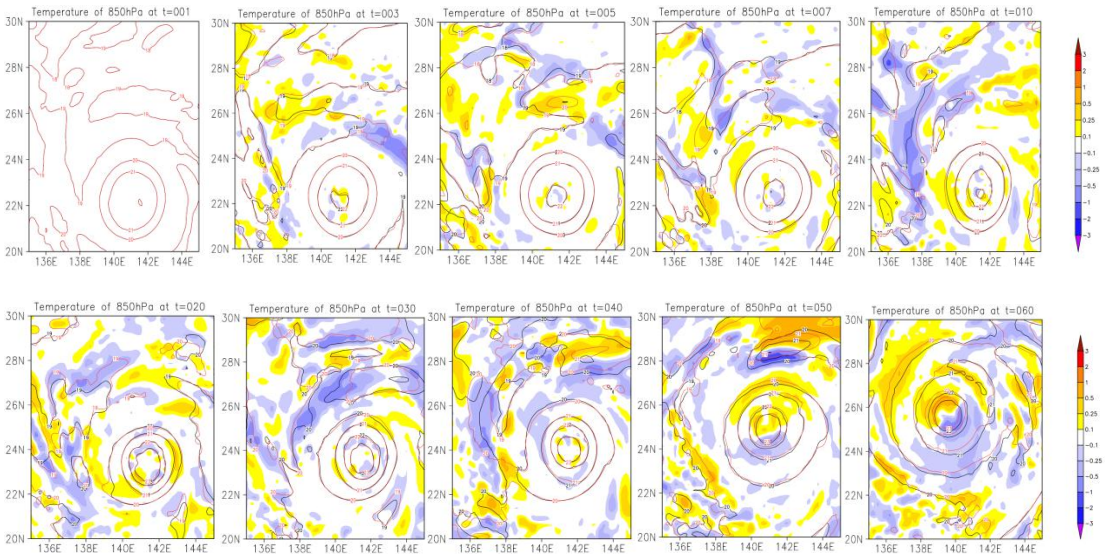

Figure R3. The temperature of 850 hPa simulated by G00 (the red line) and G21 (the black line) experiments and the difference of G00-G21 (shad) at different integration time, the unit is K.

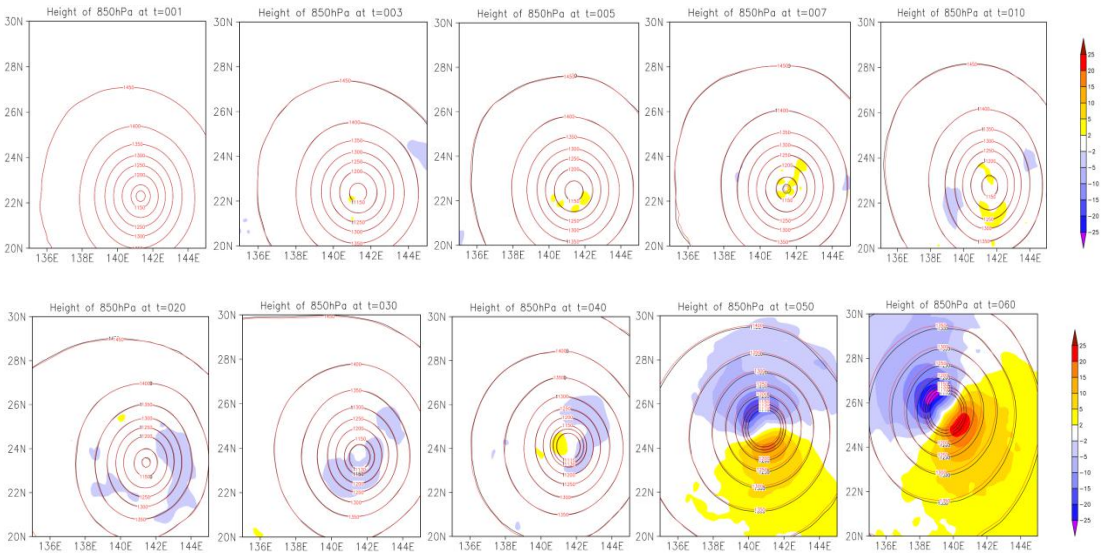

Figure R4. The geopotential height of 850 hPa simulated by G00 (the red line) and G21 (the black line) experiments and the difference of G00-G21 (shad) at different integration time, the unit is gpm.

Spin-up Characteristics with Three Types of Initial Fields and the Restart Effects on the Forecast Accuracy in GRAPES Global Forecast System

Zhanshan Ma[1,2,3], Chuanfeng Zhao[1*], Jiandong Gong[2,3], Jin Zhang[2,3], Zhe Li[2,3], Jian Sun[2,3], Yongzhu Liu[2,3], Jiong Chen[2,3], Qingu Jiang[2,3]

[1]State Key Laboratory of Earth Surface Processes and Resource Ecology, and College of Global Change and Earth System Science, and Joint Center for Global Change Studies, Beijing Normal University, Beijing, 100875, China
[2]National Meteorological Center, Beijing, 100081, China
[3] Numerical Weather Prediction Center of China Meteorological Administration, Beijing, 100081, China

Correspondence to: Chuanfeng Zhao (czhao@bnu.edu.cn)

Abstract. The spin-up refers to the dynamic and thermal adjustments at the initial stage of numerical integration to reach a statistical equilibrium state. The analyses on the characteristics and effects of spin-ups are of great significance for optimizing the initial field of the model and improving its forecast skills. In this paper, three different initial fields are used in the experiments: the analysis field of four-dimensional variational (4D-VAR) assimilation, the 3-hour prediction field in the operational forecasting system, and the Final (FNL) Operational Global Analysis data provided by National Centers for Environmental Prediction (NCEP). Then, the characteristics of spin-ups in the version 2.3.1 of GRAPES (Global/Regional Assimilation and Prediction System) global forecast system (GRAPES_GFS2.3.1) under different initial fields are compared and analyzed. In addition, the influence of the lost cloud-field information on the spin-up and forecast results of the GRAPES model in the current operation is discussed as well. The results are as follows. With any initial field, the spin-up of GRAPES_GFS2.3.1 has to go through two stages - the dramatic adjustment in the first half hour of integration and the slow dynamic and thermal adjustments afterwards. The spin-up in GRAPES_GFS2.3.1 lasts for at least 6 hours, and the adjustment is gradually completed from lower to upper layers in the model. Therefore, in the evaluation of the GRAPES_GFS2.3.1, the forecast results in the first 6 hours should be avoided. And the GRAPES_GFS2.3.1 with its own analysis field performs better than the one using FNL reanalysis data for the cold start in the spin-up, because the variations in amplitudes of the temperature and humidity tendency are smaller and the spin-up time is slightly shorter. Based on the 4D-VAR assimilation analysis field, the forecast in the operational model is artificially interrupted and restarted after 3 hours of integration. In this process, as the cloud-field information is not retained, the spin-up should repeat in the model. The characteristics of spin-up are mostly consistent with those using the 4D-VAR assimilation analysis field as the initial field. However, as the cloud-field information is not retained in the current operation, the hydrometeor content in the atmosphere at the early stage of the forecast is underestimated, affecting the calculation accuracy of the radiation and causing a systematic positive bias of temperature and

geopotential height fields at 500 hPa. ~~Besides~~In addition, the precipitation is also underestimated at the early stage of the simulation, affecting the forecast of typhoon tracks.

1 Introduction

Norwegian scholar Bjerknes (1904) first explicitly proposed the theory of numerical forecasting in the early 20th century. After more than a century of development, it has become an effective way for studying climate change and its causes, as well as forecasting climate and weather. ~~Besides~~ In addition, higher requirements have been also raised for the improvement of numerical forecast accuracy (Peter et al., 2015; IPCC 2013).

The numerical forecast accuracy is determined by a variety of factors. The European Centre for Medium-Range Weather Forecasts (ECMWF) concluded that the steady improvement of the numerical forecast in the past 30 years can be mainly attributed to the improvement of the forecast model itself, the application of more observation data, and the development of data assimilation technology (Linus & Erland, 2013). Among them, the performance of the forecast model is mainly determined by the model resolution, the accuracy of finite difference methods, and the ~~reasonability~~representativeness of the physical process parameterization schemes. Observation data mainly depends on the development of monitoring technology, especially the application of satellite data. Data assimilation integrates observation data from different sources with model forecast elements so that the observation data can be comprehensively used by the models. The main purpose of data assimilation is to create a simulated atmosphere state closer to the real atmosphere, reduce the bias of the initial atmosphere condition, and thereby improve the quality of the initial field. In data assimilation, observation data from many sources are used. The uncertainties in the observation data, the inconsistencies among observation elements, and the model flaws (caused by model dynamic assumptions, interactions between physical processes, static data initialization and the radiation balance adjustment, etc.) can lead to inconsistencies between the assimilated new observation input data and the original data in the model. Therefore, the model needs to readjust the dynamic and thermal processes at the initial stage of integration until a new statistical equilibrium state is reached. This process is called the spin-up in numerical ~~model~~modeling, and the time required to reach a new equilibrium state is called the spin-up time (Wolcott & Warner, 1981; Kasahara et al., 1992; Séférian et al., 2016; Sheng et al., 2006; Liu et al., 2008; Xue et al., 2017). During the dynamic and thermal adjustment in the spin-up, spurious gravity waves ~~could~~ can be triggered, causing a rapid increase in the root mean square error of the forecast variables in the model and an underestimation of the forecast precipitation (Wehbe et al., 2019; Qian et al., 2003). It leads to unreliable forecast results during the spin-up. Therefore, many studies generally do not consider the forecast results during the spin-up when evaluating the model forecasts (Lo et al., 2008; Kleczke et al., 2014; Xie et al., 2013; Zhao et al., 2012). If the spin-up time is too long in the operational model, it would inevitably affect the forecast accuracy of the model. In addition, the overlong spin-up in the climate model or the ocean model can consume excessive computing resources (Duben et al., 2014). Therefore, studying the spin-up characteristics and reducing the spin-up time are of great significance for improving the model forecast and saving computing resources.

Due to different types and usages of numerical models, the spin-up time in different models is greatly different. For example, in global climate models, glacial models, and ocean circulation models, the spin-ups usually take decades to hundreds of years (Scher & Messori 2019; Danek et al., 2019; Rimac et al., 2017). But in a regional climate model or a land surface model, only several weeks to several months are needed (Zhong et al., 2008; Rimac et al., 2017; Senatore et al., 2015; Giorgi & Mearns 1999; Chen et al., 1997). In addition, the spin-up time is also affected by factors such as the simulation domain, the simulation season, and the circulation intensity (Anthes et al., 1989; Errico et al., 1987). The spin-up time of short-term weather forecast models is relatively short, usually several hours to about a dozen of hours (Weiss et al., 2008; Souto et al., 2003; Kasahara et al., 1988). To reduce the impact of overlong spin-up on the accuracy of numerical forecasts, many technical methods have been developed to shorten the spin-up time. For example, the "Distorted Physics", "Matrix-method", "Jacobian-Free Newton-Krylov" are used in marine models (Bryan 1984; Khatiwala et al., 2005; Knoll & Keyes 2004). And the cloud analysis method for assimilating unconventional observation data such as satellites and radars is used in the short-term weather forecast model to improve the initial humidity field and cloud field, shorten the spin-up time, and improve the short-term precipitation forecast (Li et al., 2018; Zhu et al., 2017; Xue et al., 2017; Li et al., 2011; Zhi et al., 2010; Xue et al., 2003; Carlin et al., 2017).

The Global/Regional Assimilation Prediction System (GRAPES) is a numerical weather forecast model independently developed by the China Meteorological Administration (CMA). It has become the core of the national numerical forecast operational system in China. Numerical Weather Prediction Center of CMA has established a deterministic weather forecast model system with a global horizontal ~~resolution~~ grid spacing of 25 km and a national horizontal ~~resolution~~ grid spacing of 3 km (Shen et al., 2017; Zhang et al., 2019; Ma et al., 2018; Chen & Shen 2006). Hao et al. (2013) used the three-dimensional variational (3D-VAR) system to perform the assimilation and analysis of initial fields in the GRAPES regional model, achieving a good forecast result. The research by Zhu et al. (2017) showed that the cloud analysis method in the GRAPES regional model can effectively shorten the spin-up time. After 1-hour integration in the model, the precipitation forecast is very close to the observation, and it has a positive impact on the threat score of precipitation forecast within 12 hours. Li et al. (2011) also showed similar findings. The assimilation module of GRAPES global forecast system (GRAPES_GFS) was upgraded from 3D-VAR to 4D-VAR assimilation system in July, 2018. The analysis and forecast ability of 4D-VAR assimilation system is significantly better than 3D-VAR (Zhang L et al., 2019). However, there are still many unknowns to be answered. For example, what are the characteristics of the spin-up at the early stage of integration in GRAPES_GFS after the upgrade? ~~What advantages does it have, compared with the cold start simulation with the widely used FNL (Final Operational Global Analysis) reanalysis data provided by NCEP (National Centers for Environmental Prediction) (Kalnay et al., 1996)?~~ In the research and development of the GRAPES-GFS, the widely-used FNL (Final Operational Global Analysis) reanalysis data provided by NCEP (National Centers for Environmental Prediction) (Kalnay et al., 1996) is usually adopted as the model's initial field to quickly evaluate the effects of modification in dynamic core and physical processes on the model forecast performance, because the cold start simulation with FNL consumes less computing resources than that of cycle assimilation simulation. Then another question is what advantages the new 4D-VAR assimilation analysis fields have in spin-up process compared with the cold start simulation with FNL. In addition, we should note that each forecast result of

GRAPES_GFS is from the model integration forecast based on the 4D-VAR assimilation analysis field 3 hours ago in the current operational forecast system. For example, the 1200 UTC forecast result is based on the 4D-VAR assimilation analysis field at 0900 UTC. Actually, for numerical weather prediction model's users (especially forecasters), they are usually accustomed to referring the forecast productions of model staring to integrate from 00 UTC or 12 UTC (or more time, for example 06 UTC, 18 UTC). ~~However~~Thus, considering the habit of users ~~(especially forecasters)~~ in using the forecast results, GRAPES_GFS integrates for 3 hours (to 1200 UTC) to retain the ~~fields of basic~~essential meteorological element fields~~s~~ (U, V, T, Q, H, TS , Ps, etc.), and then the integration is terminated and restarts from 1200 UTC by using the new-saved ~~weather~~ meteorological field data. The model forecast results thereafter are released, that is, the forecast results at 1200 UTC are obtained by users. In this process, the cloud-field ~~information~~variables (the mass and concentration of hydrometeors and cloud cover) during the first 3 hours of integration ~~is~~ are not retained in the model, losing the cloud information formed after the 3-hour spin-up. The reasons for the unretained cloud-field variables were mainly based on the following considerations: the hydrometeor contents are very small amount relative to water vapor and they can be quickly created in the spin-up process when the model restarts. Moreover, this treatment can save storage space and input/output (IO) time. However, its impacts on the spin-up process and model forecast performance have not yet been carefully analyzed and evaluated. Therefore, we need to fully diagnose and analyze the necessity of the repetition of GRAPES_GFS spin-up during the re-integration, and the impact of the lost cloud-field information on the later forecast. In this regard, the characteristics of spin-ups in GRAPES_GFS respectively using the 4D-VAR analysis data and the FNL data as the initial field are compared and analyzed, and the impacts of the cloud-field information loss in the current operation on the spin-up after the model restart and on later forecast results are discussed. This paper aims to provide the scientific basis for understanding the characteristics of GRAPES_GFS at the initial stage of integration and improving the assimilation system and operational procedure.

The paper is organized as follows. In section 2, the GRAPES_GFS forecasting system and the experiment settings for one case study are introduced. In section 3, the main research results are presented. Finally, in section 4, the main conclusions are given, and some issues about spin-ups are discussed.

2 GRAPES_GFS2.3.1 and experiment setup

2.1 GRAPES_GFS2.3.1

GRAPES is a global numerical weather prediction system that is composed of atmospheric model and variational data assimilation system (3D-VAR/4D-VAR). The framework of the atmospheric model is a fully compressible non-hydrostatic dynamical one with semi-implicit and semi-Lagrangian time difference scheme. In the horizontal direction, the equidistant latitude-longitude grid system with the Arakawa-C grid and central ~~difference~~ differencing of second order accuracy for variable staggering is used; and in the vertical direction, the height-based terrain-following coordinate with the Charney-Phillips staggering is adopted. Forecast variables of GRAPES_GFS include the dimensionless air pressure (Exner function), potential temperature, three-dimensional wind field components, and specific humidity. And it introduces the Piecewise

Rational Method (PRM) scalars (Su et al., 2013) into the model, which is a scheme of water vapor advection. The physical parameterization schemes used in the GRAPES_GFS operation mainly include the long-wave and short-wave radiation scheme (the rapid radiative transfer model (RRTMG)) (Morcrette et al., 2008; Pincus et al., 2003), the land surface scheme (the Common Land Model (CoLM)) (Dai et al., 2003), the planetary boundary layer scheme (Medium-Range Forecast (MRF)) (Hong & Pan 1996), the deep and shallow cumulus convection parameterization scheme (the New Simplified Arakawa-Schubert (NSAS)) (Arakawa & Schubert 1974; Liu et al., 2015; Pan & Wu 1995). The cloud physics scheme includes the macro cloud scheme dealing with the condensation process under the unsaturated condition of grid-average water vapor, a double-moment cloud microphysical scheme, and a cloud cover prognostic scheme (Chen et al., 2007; Ma et al., 2018). ~~The 4D-VAR is adopted in GRAPES_GFS (Zhang et al., 2019).~~ On 1 July 2018, the GRAPES global 4-dimensional variational (4D-Var) data assimilation system has been in operation (Zhang et al., 2019), which is called version 2.3.1 of GRAPES_GFS (abbreviated as GRAPES_GFS2.3.1). The GRAPES_GFS2.3.1 version is adopted in this research.

~~1~~2.2 Experiment setup

In this paper, the ~~weather process in~~ GRAPES_GFS2.3.1 with the operational forecast time of 0000 UTC on August 9, 2019 is taken as an example, and three experiments are set up to analyze the similarities and differences in the spin-up characteristics of the model using different initial fields. The settings are shown in Table 1. In the first experiment, the analysis field provided by the 4D-VAR assimilation analysis system in the operational forecast at 2100 UTC on August 8, 2019 is used as the initial field to directly perform model integration forecasts, and the initial time is 2100 UTC on August 8. This experiment is called G21. ~~In the second experiment, the initial field in the operation is used, and the results are the forecast products provided by GRAPES_GFS operational system to the users. At 0000 UTC on August 9 (3 hours after the beginning of integration in G21), it retains the model variables required by the pre-processing system and stops the integration, but loses the cloud field information (e.g. hydrometeors and cloud cover). And then the model restarts at 0000 UTC on August 9 with the reserved forecast field information for forecasting. This experiment is called G00.~~ For the second experiment, called G00, its initial field adopts 3 hours integration output of G21 without retaining cloud-field information. That is to say, at 0000 UTC on August 9, it retains the G21's 3-h forecast variables (u and v wind field components, potential temperature, water vapor and dimensionless air pressure, etc.) required by the pre-processing system and stops the integration. During the process, the fields of all hydrometeor contents and cloud cover are lost considering the limitation of IO time and disk space. And then the model restarts at 0000 UTC on August 9 with the reserved forecast-field information for forecasting in G00. Moreover, the model output of G00 is exactly the forecast results to be provided to users in the GRAPES_GFS2.3.1 operation. The third experiment uses the initial field from the NCEP FNL reanalysis data at 0000 UTC on August 9, 2019 to perform integration forecast. The purpose is to compare the spin-up characteristics of GRAPES_GFS2.3.1 model respectively using its own analysis field and FNL reanalysis field as the initial field. This experiment is called F00. To analyze the impacts of the initial field on the forecast, G00 and F00 produce a continuous 72-hour forecast. As G21 starts the integration 3 hours earlier than the other two, the forecast of G21 lasts for 75 hours to ensure the same forecast and analysis period with G21 and G00.

All the three experiments are based on the GRAPES_GFS2.3.1 operational model, with a horizontal ~~resolution~~ grid spacing of 0.25°, 60 vertical layers, and a model integration time step of 300 s. The physical schemes used are from the operational ~~solutions~~ setup (as described in section 2.1), and the assimilation module is 4D-VAR assimilation system. To explicitly analyze the spin-up characteristics of the GRAPES_GFS2.3.1 at the early stage of integration, the results of each integration step are ~~outputted~~-output, and the temperature tendency (TT) and water vapor tendency (WVT) fields at each model layer during the dynamic and physical processes are retained.

In addition, the cloud-field information has not been saved during the restart in the current operation. To examine its impact on the accuracy of the later forecast, this study investigates the Super Typhoon "Lekima" (No. 1909) that landed on China during the selected forecast period, and the forecast differences in cloud, precipitation field and typhoon track during "Lekima" between G00 and G21 are analyzed.

3 Results

3.1 Characteristics of spin-ups

3.1.1 Characteristics of total WVT and total TT

To analyze the spin-up characteristics of GRAPES_GFS2.3.1, the initial fields in F00, G21, and G00 are used to perform the integration, and the temporal variations of the average total WVT and TT at different heights from 0000 UTC to 1200 UTC are calculated, as shown in Fig. 1. Seen from the figure, both the WVT and TT show sharp fluctuations at the initial stage of the integration in the three experiments, especially during the first hour. After 3–6 hours of spin-up adjustment, the variation magnitudes of WVT and TT become gradually gentle, but the variation characteristics vary with different initial fields. At the early stage of the integration, the WVT is adjusted in F00 and G21, with the amplitude of -4.5 g kg^{-1} d^{-1}. In G21, the water vapor adjustment occurs in the lower layers of the model (850 hPa and 925 hPa), while the WVT is relatively gentle without an obvious adjustment in the upper and middle layers (500 hPa and 300 hPa). In F00, the water vapor adjustment occurs at the upper levels of the model at the early stage of integration. The WVT at 300 hPa can reach -4.5 g kg^{-1} d^{-1}, but it weakens immediately afterwards, probably due to the supersaturated water vapor in the initial field from FNL data. In F00, the WVT in the lower layers of the model is also significantly larger than that in G21. For example, at 850 hPa, the WVT in F00 maintains about 1 g kg^{-1} d^{-1} for relatively long time, but that in G21 mostly changes within 0.5 g kg^{-1} d^{-1}. The corresponding temperature adjustment processes in the two experiments present the same variation characteristics as the WVT adjustment. Therefore, the spin-up in the integration using the analysis field of GRAPES_GFS2.3.1 as the initial field is gentler than that using the FNL reanalysis data as the initial field.

In G21 and G00, both the variations of WVT and TT are very consistent, indicating that G00 has well inherited the temperature and humidity structure of G21. However, G00 still needs to go through the spin-up during which a gradually stable adjustment process follows a sharp fluctuation at the early stage of integration, that is, the dynamic and thermal adjustments are required

to reach a statistical equilibrium state in the model. At the initial stage of integration in G00, the variation amplitudes of WVT and TT are smaller than those in G21, but greater than those in G21 after the 3-hour integration. It shows that although G00 can retain the temperature and humidity structure of G21, the loss of cloud-field information in the operation still has a destructive effect on the model equilibrium state after 3-hour adjustments. Based on the variation of TT, the spin-up time required for G00 is generally less than that for G21. It takes about 6 to 8 hours to reach a TT equilibrium state in G21, but it is less than 6 hours in G00.

3.1.2 Tendency characteristics of the model dynamical and physical processes

In the GRAPES_GFS2.3.1, the total temperature tendency of the model (ALL) is determined by dynamic core (DYN), radiation process (RAD), turbulent mixing in planetary boundary layer process (PBL), cumulus convection process (CONV) and cloud physical process (CLOUD). Among them, the total temperature tendency of all physical processes (PHY) is defined as the sum of the last four items (PHY=RAD+PBL+CONV+CLOUD). Likewise, the total water vapor tendency for ALL and PHY are same to those of temperature tendency except for the radiation process (RAD). Fig. 2 shows the temporal variation of mean WVT ~~in the~~due to dynamic and physical processes at different heights in F00, G21 and G00. In the middle and upper layers of the model (Figs. 2a and 2d), there is a drastic adjustment in the atmosphere at the early stage of the integration in F00. It may be due to the supersaturated water vapor in the initial field from FNL data, which causes the cloud to condense very quickly, and thus a relatively stable state is reached, after three integration steps. ~~At this level in G21, the WVTs at the first few integration steps are slightly larger than that at the subsequent integration steps, while the variation of water vapor is mainly caused by the co-action of cloud and convections.~~ At these levels in G21 (Figs. 2b and 2e), the total WVTs at the first few integration steps are slightly larger than that at the subsequent integration steps. The variations of the WVTs from dynamic core and turbulent mixing process in the planetary boundary layer are much less than those from the cumulus convection process and cloud physical process, and the latter two processes jointly determined the variation of WVTs at 300 hPa and 500 hPa. There is not much difference in the dynamic field tendencies between G21 and F00. The magnitudes of the WVTs in the dynamic processes of the two experiments are also very close: around 0.5 g kg^{-1} d^{-1} at 500 hPa and 0.25 g kg^{-1} d^{-1} at 300 hPa. Therefore, the differences of the upper-middle-level water vapor adjustments in the spin-ups between G21 and F00 are mainly caused by physical processes, and there is a good consistency in the dynamic process between the two experiments. At 925 hPa (the lower layer of the model), the total WVT stays around 1 g kg^{-1} d^{-1} in F00 after three integration steps, humidifying the atmosphere. In G21, it reaches a relatively stable state after six integration steps, and water vapor decreases overall. As the WVTs of the dynamical processes in F00 and G21 have the same magnitude around 0.25 g kg^{-1} d^{-1}, the difference of the total WVT between G21 and F00 is mainly caused by physical processes. The effect of the boundary layer on the WVT is similar in both experiments and the WVT is almost 3 g kg^{-1} d^{-1}. The greatest difference between the two experiments is mainly caused by the convection scheme. The convection in F00 is relatively gentle, and the WVT from convection is around -1 g kg^{-1} d^{-1}. In contrast, due to the strong dehumidification ability of ~~convections~~ convection- in G21, the WVT is between -5 g kg^{-1} d^{-1} and -2.5 g kg^{-1} d^{-1}, which is significantly stronger than that in F00. At 925 hPa, the water vapor mainly decreases due to the

strong convection process in G21. Such a significant difference in the convection processes between F00 and G21 may be related to the low-level temperature and humidity structures and the triggering conditions for ~~convections~~convection-. Meanwhile, it can be seen that the difference in the initial field of the model can significantly affect the physical processes.

In summary, in the middle and upper atmosphere, the fluctuation of WVT in G21 is weaker than that in F00, indicating the advantage of using the data assimilation cycling as the initial field. Both experiments quickly reach a quasi-equilibrium state after dramatic adjustments over several integration steps. The water vapor adjustment in spin-ups mainly occurs in the lower atmosphere of the model. The difference is mainly caused by different convection schemes. At the same time, different initial fields of the temperature and humidity structure may lead to a great difference in the dehumidification ability of ~~convections~~convection-. For G00 and G21, the WVTs of the dynamic and physical processes have roughly the same characteristics. At all of the three levels, the WVTs in G00 are slightly lower than those in G21.

In the middle and upper layers of the model, the dramatic change of the TT in F00 mainly occurs within the first half hour of the integration (Figs. 3a and 3d). ~~The TT in the physical process is mainly caused by the water vapor condensation due to the cloud and convection processes (Fig. 2). Compared with the convection process, the cloud physical process can cause greater temperature adjustments.~~ Among all the TTs at the first integration step, the cloud physical process leads to the largest one, followed by convection process, and they are related to the water vapor condensation process (Figs. 2a and 2d). For example, at 500 hPa, the global average heating produced by the cloud microphysical condensation process at the initial time can exceed 5 K d^{-1} and it takes four integration steps to reach a relatively stable state. But at this level, the TT caused by the convection process is 3 K d^{-1}, and it only needs one integration step with the drastic adjustment to get relatively stable. In addition, the TT caused by the dynamic process fluctuates greatly at the first half hour of the integration. For example, at 300 hPa, the TT fluctuates between 1.1 K d^{-1} and 1.5 K d^{-1}, and it requires extra 3 or 4 integration steps to reach a relatively stable state compared to the physical processes. Nevertheless, after half an hour of severe fluctuations, the TT caused by dynamic and physical processes tends to be relatively stable. Overall, the temperature increases by 0.25 K d^{-1} to 0.5 K d^{-1} in the middle and upper atmosphere in F00. Compared with that in middle and upper layers, the TT variation caused by the dynamic and physical processes in the lower layer of the model (Fig. 3g) shows a relatively ~~large~~ small and rapid adjustment at the first integration step. But no drastic adjustment is shown afterwards, and its variation is relatively stable. ~~The TT at 925 hPa in F00 is mainly caused by dehumidifying and heating of the atmosphere from the convection parameterization. The average global heating is between 1.5 K d^{-1} and 2 K d^{-1}. The TTs caused by other processes are negative. Overall, in F00 the atmospheric temperature is reduced at 925 hPa, with an amplitude of about -1.2 K d^{-1}.~~ The TT of the convection process at 925 hPa in F00 varies between 1.5 K d^{-1} and 2 K d^{-1}, which is mainly caused by condensing and dehumidifying of the atmosphere (Fig. 2g). Except for the cloud physical process with a relatively small positive tendency in the first four time steps, the TTs of dynamic core and other physical processes are all negative. Overall, in F00 the total atmospheric temperature is reduced with an amplitude of about -1.2 K d^{-1} in the first hour of the integration at 925 hPa.

In G21, the TT in the middle and upper layers also experiences a dramatic adjustment in the first half hour of the integration (Figs. 3b and 3e), and the main reason for the fluctuation is the dehumidification and heating in the convection process, which is different from that in F00 caused by the cloud physical process. The temperature increase caused by the convection process in G21 is 1 K d^{-1} to 2.5 K d^{-1}, which is about twice that in F00. The TT caused by the cloud physical process in G21 varies relatively gently. Similar to F00, the TT caused by the dynamic process in G21 also shows obvious fluctuations, which may be caused by the drastic variations of physical processes. In the lower layer of 925 hPa (Fig. 3h), the positive TT in G21 is also caused by convective dehumidification and heating, while other processes lead to cooling. In terms of the total TT (dynamic core plus all physical processes), F00 has a cooling effect with a value of -1 K d^{-1}, while G21 has a warming effect with a value within 1 K d^{-1}. The temperature increase rate of G21 gradually decreases with the integration step.

The characteristics of the TT variation in G00 are consistent with those in G21 (Figs. 3c, 3f and 3i). ~~In the first half hour, it also has a drastic adjustment process, with the adjustment amplitude close to or slightly smaller than those in G21.~~ In the first few time steps, G00 also has an adjustment process, with the adjustment amplitudes of TT close to half those in G21 at all levels. After half an hour, the temperature tends to be relatively stable. The TT variation in G00 indicates that although G21 has undergone a 3-hour spin-up, G00 needs to undergo it again due to the loss of cloud-field information during the restart, and its fluctuation amplitude is not substantially smaller than that of G21.

3.1.3 Evolution characteristics of the cloud field

The comprehensive adjustment effect of the dynamic and the physical processes on the water vapor and temperature in the numerical model can be presented by the cloud state. To reveal the dynamic and thermal adjustment processes in GRAPES_GFS2.3.1 system at the beginning of the integration and the time required for the ~~analysis~~ model to reach the statistical equilibrium state (spin-up time), this section uses the total grid number of cloud (TGNC) in the model as the index for analyses. Although the cloud is changing locally, the total area covered by cloud can be regarded as a constant globally on average. Therefore, TGNC is used as the analysis index, and the model is considered to have completed the spin-up when the TGNC gets relatively stable. The total hydrometeors content (THC, THC = cloud water + raindrop + cloud ice + snow + graupel) greater than 1.0 e-4 g kg^{-1} in GRAPES_GFS2.3.1 is defined as the grid with cloud, and the TGNC at a global scale or a certain height is the sum of all the grids in the corresponding cloud area.

Fig. 4 shows the vertical distributions of TGNC at different lead time in three experiments. It can be seen that ~~no matter the~~ regardless of whether the GRAPES_GFS2.3.1 model is cold-started with reanalysis data (F00, Fig. 4a) or warm-started with the 4D-VAR analysis field as the initial field (G21, Fig. 4b), the TGNC experiences rapid generation and growth during the 3 hours after the beginning of integration in the two experiments, especially in the middle- and low-cloud regions below 300 hPa. After 3 hours of integration, the TGNC grows relatively slowly, while after 6 hours of integration, the TGNC basically gets stable. However, the time required for the TGNC to reach the equilibrium state is slightly different at different heights. In F00, the integration time required for the TGNC to gradually reach the statistical equilibrium state below 850 hPa is 6 hours. ~~Note that the statistical equilibrium state is defined when the difference between the TGNC after 24 hour integration below~~

~~850 hPa and the TGNC after 6-hour integration is insignificant.~~ Note that the statistical equilibrium state is defined when the difference of TGNC with respect to the 24-hour integration is insignificant (the difference is less than 20% of TGNC at 24-hour). However, it takes 6–12 hours for the TGNC to get stable and completes the spin-up above 850 hPa. For G21, the TGNC of the middle and low cloud below 300 hPa needs 6 hours to reach the statistical equilibrium state, while the TGNC of the high cloud above 300 hPa needs 6–12 hours. It can be seen that the GRAPES_GFS2.3.1 using the analysis field from its own data assimilation cycling enables the cloud field in middle and upper layers to reach the equilibrium state earlier than that using FNL data for the cold start. In addition, GRAPES_GFS2.3.1 is gradually adjusted from the lower to the upper layers of the model to reach the equilibrium state, which is consistent with the evolution characteristics of the thermodynamic process in the troposphere. For the cloud above 500 hPa, the TGNC in F00 is significantly more than that in G21, which is related to a higher relative humidity of the initial field ~~(Fig. 6)~~. Compared with G21, F00 has a wetter water vapor environment at the upper levels (Fig.6d), which tends the water vapor to quickly condense into more hydrometeors through cloud scheme to eliminate supersaturated water vapor at the beginning of the integration (Fig.2a). Thus F00 has a higher hydrometeor content value and a wider distribution of cloud region (Figs.5a and 5e) and its TGNCs are also larger than those of G21 at the upper layers.

In G00 (Fig. 4c), the growth of TGNC is found to be much slower than that in G21, especially the TGNC of the middle and upper cloud. For example, at time 3 hours after the beginning of G00, the TGNC of the middle cloud is mostly between 15 and 20, while the TGNC in G21 can reach 25–30. The reason may be that the humidity and temperature fields of the model in G21 are already in a relative equilibrium state after 3-hour spin-up. Meanwhile, as the restart of GRAPES_GFS2.3.1 has lost the cloud-field information (light blue dotted line) from the 3-hour integration, the TGNC cannot reach the previous magnitude in the middle and upper layers even if it has been integrated for 24 hours in G00 (Fig. 4c, solid purple line).

Fig. 5 shows the distributions of THC at 400 hPa at different ~~lead~~ forecast time in the three experiments. It can be seen that the temporal variation characteristics of THC and its horizontal distribution at 400 hPa have consistent results with those shown in Fig. 4. In F00 and G21, as supersaturated water vapor is removed from the initial field, the cloud is quickly generated at the first integration step of the model. The THC rapidly increases within 1 hour, and the cloud area with high hydrometeor content is constantly expanding. For example, ~~at time 1 hour after~~ at 1 hour into the integration in F00, the THC in most areas of the Pacific Warm Pool is 0.2 g kg^{-1}. With the further adjustment of the spin-up, the THC in this area gradually decreases, and maintains a relatively equilibrium state after 6 hours of integration. The variation characteristics of the THC in the storm track area (60°S–30°S) in the southern hemisphere are similar to those in the warm pool area, but less significant.

Experiments using the 4D-VAR analysis field to provide the initial field (Figs. 5e–5h) show that the variation characteristics of THC at 400 hPa are generally consistent with those in F00. After the first integration step of GRAPES_GFS2.3.1, cloud areas are quickly generated in tropical and mid-latitude areas. Due to the rapid development of convection processes in tropical areas, more cloud with THC of 0.0–0.05 g kg^{-1} appears. After 3 hours of integration, the development of the cloud area gradually weakens. After 6 hours of integration, the variations of the range and shape of the cloud area are no longer obvious, and it can be considered that a relatively equilibrium state is reached. From the view of absolute value of THC in the cloud

area, although the difference in the distribution range of the cloud is insignificant, the THC in G21 is significantly less than that in F00 due to the different temperature and humidity conditions in their initial fields (Fig. 6).

Since G00 does not retain the cloud-field information after 3 hours of integration in G21 (the THC in Fig. 5g), the model needs to undergo a new cloud-generation process when restarting the integration. However, as the dynamic and thermal fields are obtained after 3 hours of adjustments in G21, the relative humidity has undergone a condensation process, making the atmosphere of G00 with much weaker supersaturation at initial time than that in G21 ~~at initial time~~. Therefore, unlike F00 (Fig. 5a) or G21 (Fig. 5e), in which large-scale cloud appears instantaneously, the cloud field in G00 can only be gradually generated by the dynamic and physical processes of the model. It can be seen from Figs. 5i–5k that this process is relatively slow, and a relatively stable cloud distribution does not appear until 3 hours after the integration. The cloud range in G00 at that time is smaller than that in G21, and it generally reaches the equilibrium state after 6 hours of integration. The influence of slower generation and smaller range of the cloud in G00 on the model forecast results will be analyzed and explained in section 3.2.

To reveal the reason why the TGNC (Fig. 4) and the THC (Fig. 5) in the upper layers of the model in F00 are significantly higher than those in G21, the difference of water vapor content and relative humidity at 400 hPa is analyzed, and the results are shown in Fig. 6. Fig. 6c shows that the specific humidity in the initial field of F00 is generally higher than that of G21 in the tropical areas and the middle and high latitude areas of northern hemisphere, especially in the tropical warm pool area where the difference is mostly over 0.2 g kg^{-1}. The relative humidity ~~can reflect~~ reflects the degree of water vapor saturation. Fig. 6d shows that the ~~relative~~ humidity of the initial field from the FNL reanalysis data is relatively higher than that from the 4D-VAR analysis field in the tropical warm pool, Intertropical Convergence Zone (ITCZ), and middle and high latitude areas at 400 hPa. ~~It~~ This means that the water vapor is more likely to get saturated using the FNL reanalysis data as initial field. Thus, the cloud area is larger and the THC is higher at the beginning of the integration. It is not difficult to conclude that there are differences in the structure of atmospheric temperature and humidity among different initial field data, which significantly impacts the spin-up characteristics of the model as well as the cloud formation and development. It also suggests that we need to pay more attention to the analysis quality of water vapor in data assimilation (DA). And this has been also confirmed by previous studies (Weygandt et al. 2002; Ge et al. 2013) that the accurate moisture initial field by DA is an effective way to improve the forecast performance of supercell storm in numerical weather prediction models.

3.2 Impacts on later forecast results

It can be seen from section 3.1 that the cloud-field information formed in the first 3 hours of integration has not been saved ~~in the operation~~ operationally, so the model must restart the spin-up, and THC appears to be significantly less in the new spin-up. In order to discuss the impact of the restarted spin-up and the ~~less~~ decreased THC on the later forecasts by GRAPES_GFS2.3.1, the global radiation field and synoptic ~~situation~~ field (temperature and geopotential height) are analyzed in this section. The cloud and precipitation fields and the ~~typhoon~~ track of the super typhoon "Lekima" that ~~landed on~~ made landfall in China during the simulation period will be analyzed as well.

3.2.1 Impacts on global radiation

Fig. 7 shows the zonal mean distributions of averaged column cloud water content (CCWC), the outgoing longwave (OLR) at the atmosphere top and the downward longwave at ground (GDLW) simulated by G21 and G00 from 0000 UTC to 0300 UTC on August 9, 2019, as well as the distributions of difference between them. It can be seen from Fig. 7a that the total zonal-averaged CCWC forecasted in G00 is systematically smaller than that forecasted in G21. The areas with smaller CCWC are mainly located in the Southern Hemisphere storm track, tropical low-latitude areas, as well as middle- and high-latitude areas in the northern hemisphere with active cloud. Among them, the area with the smallest CCWC is the active area of Southern Hemisphere storm track, with the CCWC difference reaching 240 g m^{-2}, and there are also some areas with the CCWC difference over 200 g m^{-2} in the northern hemisphere. From the OLR and GDLW predicted in the two experiments, it can be seen that the OLR predicted in G00 is systematically larger than that in G21, with the maximum bias (20 W/m^2/s) appearing in the Southern Hemisphere storm track. This is due to the interaction between clouds and radiation, as well as the underestimation of the CCWC. In terms of GDLW, the reduced CCWC weakens the atmospheric warming effect, resulting in systematically smaller GDLW in G00 than in G21. In most areas, the GDLW is smaller than the observation by over 10 W m^{-2} s^{-1}, and the regions with the largest bias are the middle- and high-latitude areas of the Southern Hemisphere and high-latitude areas of the Northern Hemisphere.

3.2.2 Impacts on the global temperature and geopotential height fields

The change in the calculation of the radiation flux induced by cloud would seriously affect the atmospheric temperature field and geopotential height field. Fig. 8 shows the difference distributions of the 500-hPa temperature field and the geopotential height field at ~~two~~ four lead time between G00 and G21. It can be found that as there is less hydrometeor in the cloud in G00 than in G21, the temperature field in G00 at different forecast ~~moments~~ times shows a systematic warming of more than 0.1 K in the tropical low-latitude and middle-high-latitude areas with active cloud. With the increase of the lead time, the warming area is expanding and the degree of warming gradually increases. For example, after 72 hours of integration, the warming in many areas is larger than 0.2 K, and it can reach 0.5 K in some areas. Systematic biases also appear in the corresponding geopotential height field. Compared with those in G21, the geopotential height fields in G00 have also systematic positive biases. For example, in the first 24 hours of integration, the systematic biases in the geopotential height field are above 0.5 gpm, and the positive bias can exceed 1 gpm in areas with active cloud. After 72 hours of integration, the geopotential height field in the tropical area still shows a systematic positive bias, while in the middle- and high-latitude areas, the bias of the geopotential height field shows the structure with an alternation of positive biases and negative biases due to the biases of the weather system location predicted in the two experiments, but in most areas the forecast fields are still higher than the observation.

3.2.3 Impacts on typhoon forecasts

This section analyzes the biases of the cloud field, precipitation field, and the track of the Super Typhoon "Lekima" (No. 1909) and Typhoon "Krosa" (No. 1910) in 2019 during the forecast period to evaluate the impact of the lost hydrometeor information on typhoon forecast operation in GRAPES_GFS2.3.1. During the forecast, "Lekima" and "Krosa" appear as double typhoons in the western Pacific. "Lekima" ~~landed on~~ made landfall in North China ~~from offshore areas~~, while "Krosa" ~~continued to develop on ocean~~remained offshore. ~~G00 and G21 give the same forecasts for the cloud and precipitation fields of "Lekima" and "Krosa".~~Since the conclusions for both “Lekima” and “Krosa” are the same, only “Lekima” will be presented in this study. Here, we ~~only~~ show the impact on the cloud and precipitation of "Lekima" by the lost hydrometeor information on typhoon forecast operation of GRAPES_GFS2.3.1. In the last part, the path-forecast biases for the two typhoons are both given.

Fig. 9 shows the evolutions of the averaged CCWC and ~~total content of ice water~~column cloud ice content (~~TCIW~~CCIC) within the main cloud area of "Lekima" (117°E–130°E, 22°N–34°N) simulated in G00 and G21 from 0000 UTC on August 9 to 0000 UTC on August 10, 2019. It can be seen that the CCIC~~TCIW~~ predicted in G00 at the early stage of integration is obviously underestimated. The averaged CCIC~~TCIW~~ values in G21 are maintained within 850–1000 g m^{-2} from 0000 UTC to 0900 UTC on August 9, while the CCIC~~TCIW~~ is only 480 g m^{-2} at the initial time of G00. G00 needs to restart the spin-up. During the spin-up, the CCIC~~TCIW~~ predicted in G00 increases rapidly, with the greatest ~~strengthening~~ increase during 0000 UTC to 0600 UTC. After 3 hours of the integration, the CCIC~~TCIW~~ increases rapidly from 480 g m^{-2} to 820 g m^{-2}. After 6 hours of integration, the CCIC~~TCIW~~ is close to 900 g m^{-2}. In G00, the CCIC~~TCIW~~ is not as large as that in G21 until 9 hours after the beginning of integration.

Fig. 10 shows the difference distributions of both 3-hour and 24-hour accumulated precipitation (since 0000 UTC August 8, 2019) of "Lekima" between forecasts of G00 and G21.The most significant difference of the 3-hour cumulated precipitation appears within the first 3 hours of integration in G00. The 0000 UTC–0300 UTC precipitation forecasted in G00 presents a systematic underestimation when compared with G21, and the biases are all above 1 mm. The precipitation bias in the center of "Lekima" can even exceed 5 mm (Fig. 10a). As shown in Fig. 9, after 3 hours of adjustments, the total CWP and CCIC~~TCIW~~ in the typhoon system in G00 grow rapidly and gets close to the magnitudes ~~of them~~ in G21. Therefore, the difference of the 3-hour precipitation between forecasts of G00 and G21 is no longer significant during 0300 UTC–0600 UTC and 0600 UTC–0900 UTC, and there is no more systematic bias (Figs. 10b and 10c). The phase differences of the weather system lead to the structure with ~~an alternation of~~alternating positive biases and negative biases for the precipitation difference.

It can be found from Fig. 10d that the lack of cloud-field information has a significant impact on the simulation of the accumulated precipitation in the first 24 hours of "Lekima". The negative biases dominate the central area of the typhoon, that is, there is an underestimation of precipitation with the maximum bias of 5–10 mm. ~~While~~ In contrast, in the spiral cloud zone around the typhoon, there is a structure with an alternation of positive and negative biases, which is related to the location bias of the weather system simulated in the two experiments in this area.

Fig. 11 shows the forecast track evolution of "Lekima" and "Krosa" in G00 and G21 within the lead time of 72 hours. Overall, G21 performs better than G00 in predicting the tracks of these two typhoons, and there are different characteristics for the track forecast biases of the two different typhoons. "Lekima" landed on the coast of Chengnan Town, Wenling City, Zhejiang Province at 1545 UTC on August 9, 2019. There is not much difference in biases of the track forecast between G00 and G21 before "Lekima" landing. ~~While~~ In contrast, the biases appear to be different after the landfall (1600 UTC), and the track forecast in G21 is slightly better than that in ~~G20~~ G00 around the landfall. After the landfall, the track biases change continuously during the 27th to 42th hour and 54th to 60th hour of the forecast, the track bias in G21 is smaller than that in G20. The maximum difference between the two track forecasts can reach 32 km. From the 65th to 72th hour, the forecast track bias in G21 is slightly larger. For "Krosa", during the first 42 hours, the biases of the tracks forecasted in G00 and G21 are not much different. But the forecast tracks of the two become different after the 42th hour, with the track bias in G00 becoming larger. In most forecasts after the 42th hour, the track biases in G00 are over 20 km and larger than those in G21.

Overall, G21 performs better than G00 in the track forecasts of "~~Lichma~~Lekima" and "Krosa" within the lead time of 72 hours, especially in the forecast of "Krosa". For "Krosa", the forecast track on the ocean is less affected by other factors, so the forecast track biases at the later stage of the forecast are significantly smaller. It shows that GRAPES_GFS2.3.1 performs better in continuous-integration forecasts, and the interruption in the operation is destructive to the typhoon track forecast.

4 Conclusions and discussion

To analyze the characteristics of the spin-up at the early stage of integration in GRAPES_GFS2.3.1, this study adopted three different initial fields, namely the 4D-VAR analysis field (G21), the field obtained by interrupting and restarting the 4D-VAR analysis field after 3 hours of integration (G00), and the field based on FNL reanalysis data for cold start (F00). Moreover, the differences between G00 and G21 on the later model forecast results were analyzed to evaluate the impact of current operational procedure on GRAPES_GFS2.3.1 forecasts. The main conclusions are as follows.

All ~~the~~ three ~~different~~ experiments using different initial fields show that the spin-up of GRAPES_GFS2.3.1 has to go through 2 stages: the dramatic adjustment in the initial half-hour of integration and the slow dynamic and thermal adjustment afterwards. In the middle and lower layers of the model, the spin-up takes 6 hours to reach the equilibrium state, and takes longer in the upper layers. The dynamic and thermal adjustment is gradually completed from the lower to the upper layer of the model.

The GRAPES_GFS2.3.1 using its own analysis field as the initial field (G21) is gentler in the water vapor and temperature adjustment in the spin-up than the GRAPES_GFS2.3.1 using FNL reanalysis data for cold start (F00), and the time required is slightly shorter. Due to the different structures of temperature and humidity in the two initial fields, the differences of physical processes in the model spin-up adjustment are obvious, especially the convections and cloud physical processes. However, the differences in dynamic processes are ~~unobvious~~not obvious. G00 needs to repeat the spin-up. Its dynamic and thermal adjustments are similar to that in G21. The temperature and humidity adjustment in G00 is slightly weaker than that in G21, and its spin-up is slightly shorter.

In G00, the cloud-field information is not retained during the current operation of GRAPES_GFS2.3.1. It shows that G00 significantly underestimates the atmospheric CCWC and CCIC~~TCIW~~ at the early stage of forecast, which would affect the calculation accuracy of radiation and result in systematic positive biases in temperature and geopotential height fields at 500 hPa. Due to the lack of cloud-field information, the accumulated precipitation in the first 3 hours of integration in G00 is significantly underestimated. The 24-hour accumulated precipitation in the typhoon center is also less than that in G21, and a destructive effect is made on the typhoon track forecast.

Regarding the influence of the lost cloud-field information in the GRAPES_GFS2.3.1 operation on the forecast results, this paper mainly analyzes the differences of simulation results between G21 and G00, and evaluates the possible changes brought to the GRAPES_GFS2.3.1. But an in-depth analysis of how the simulation results can improve the forecast performance is absent in this paper. The reason is that the forecast biases of the numerical model result from a combination of various factors, and it is difficult to explain the improvement of the GRAPES_GFS2.3.1 forecast system just with a single case. Therefore, a batch of experiments are needed later in our future study. Since the absence of cloud-field information at a single time can bring systematic biases to the simulated temperature field and geopotential height field, in the cycling numerical forecasting operational system, the cloud-field information that has formed should be retained as much as possible. Moreover, the temperature and humidity structure in the initial field, especially the water vapor, can significantly affect the dynamic and physical processes in the numerical model. Thus, in addition to the improvement of dynamic and physical processes, more attention should be paid to the assimilation of water vapor data, to improve the data quality of water vapor in the initial field of GRAPES_GFS2.3.1.

Code and data availability. The model simulation data used in this study is available at https://pan.baidu.com/s/1QwBbw7PKQ6e8gZTbYhx9iA with access code zkuo; the model code cannot be distributed due to the copyright licence requirement from ~~is only available by request via mazs@cma.gov.cn due to the confidential requirement~~.the Numerical Weather Prediction Center of China Meteorological Administration (NWPC/CMA). If someone wants to use the GRAPES_GFS model or reproduce these experiments in this article, he/she can contact the operational management department of NWPC/CMA via email songzx@cma.gov.cn or phone +86-10-68400477.

Author contribution. ZSM and CFZ designed the experiments and ZSM carried them out. ZSM developed the model code and performed the simulations. ZSM prepared the manuscript with contributions from all co-authors.

Competing interests. The authors declare that they have no conflict of interest.

Acknowledgments

This study was supported by the National Key R&D Program on Monitoring, Early Warning and Prevention of Major Natural Disasters (grant 2017YFC1501406~~ and 2017YFC1501403~~), the National Natural Science Foundation of China (grants

41925022, 91837204, 41575143), the State Key Laboratory of Earth Surface Processes and Resource Ecology, and the Fundamental Research Funds for the Central Universities. We thank Nanjing Hurricane Translation for reviewing the English language quality of this paper.

References

Anthes, R. A., Kuo, Y., Hsie, E., Low-Nam, S., and Bettge, T. W.: Estimation of skill and uncertainty in regional numerical models, Quart. J. Roy. Meteor. Soc., 115, 763-806, https://doi.org/10.1002/qj.49711548803, 1989.

Arakawa, A., and Schubert, W. H.: Interaction of a cumulus cloud ensemble with the large-scale environment, Part I, J. Atmos. Sci., 31, 674–701, https://doi.org/10.1175/1520-0469(1974)031<0674:IOACCE>2.0.CO;2, 1974.

Bauer, P., Thorpe, A., and Brunet, G.: The quiet revolution of numerical weather prediction, Nature, 525, 47-55, https://doi.org/10.1038/nature14956, 2015.

Bjerknes, V.: Das Problem der Wettervorhersage, betrachtet vom Standpunkte der Mechanick und der Physik [The problem of weather prediction as seen from the standpoint of mechanics and physics], *Meteorologicsche Zeitschrift*, 21, 1-7, 1904.

Bryan, K.: Accelerating the convergence to equilibrium of ocean-climate models, J. Phys. Oceanogr., 14, 666-673, https://doi.org/10.1175/1520-0485(1984)014<0666:ATCTEO>2.0. CO;2, 1984.

Carlin, J. T., Gao, J., Snyder, J. C., and Ryzhkov, A. V.: Assimilation of Z_{DR} columns for improving the spinup and forecast of convective storms in storm-scale models: proof-of-concept experiments, Mon. Weather Rev., 145, 5033-5057, https://doi.org/10.1175/MWR-D-17-0103.1, 2017.

Chen, D. H., and Shen, X. S.: Recent progress on GRAPES Research and Application [in Chinese], J. Appl. Meteorol. Sci., 17(6), 773-777, 2006.

Chen, F., Janjic, Z., and Mitchell, K.: Impact of Atmospheric Surface-layer Parameterizations in the new Land-surface Scheme of the NCEP Mesoscale Eta Model, Bound.-Lay. Meteorol., 85, 391-421, 1997.

Chen, X. M., Liu, Q. J., Zhang, J. C.: A numerical simulation study on microphysical structure and cloud seeding in cloud system of QiLian Mountain Region [in Chinese], Meteorol. Mon., 33(7), 33–43, 2007.

Dai, Y., Zeng, X., Dickinson, R. E., Baker, I., Bonan, G. B., Bosilovich, M. G., Denning, A. S., Dirmeyer, P. A., Houser, P. R., Niu, G., Oleson, K. W., Schlosser, C. A., and Yang, Z.: The Common Land Model, B. Am. Meteorol. Soc., 84(8), 1013-1023, https://doi.org/10.1175/ BAMS-84-8-1013, 2003.

Danek, C., Scholz, P., and Lohmann, G.: Effects of High Resolution and Spinup Time on Modeled North Atlantic Circulation, J. Phys. Oceanogr., 49, 1159-1181, https://doi.org/10.1175/JPO-D-18-0141.1, 2019.

Düben, P. D., McNamara, H., and Palmer, T. N.: The use of imprecise processing to improve accuracy in weather & climate prediction, J. Comput. Phys., 271, 2-18, https://doi.org/10.1016/j.jcp.2013.10.042, 2014.

Errico, R., and Baumhefner, D.: Predictability Experiments Using a High-Resolution Limited-Area Model, Mon. Weather Rev., 115, 488-504, https://doi.org/10.1175/1520-0493(1987)115<0488:PEUAHR>2.0.CO;2, 1987.

Hao, M., Zhang, H., Tao, S., Gong, J.: Application of Variational Quality Control to Regional GRAPES-3DVAR [in Chinese], *Plateau. Meteorol.*, 32(1), 122-132, 2013.

Hong, S. Y., and Pan, H. L.: Nonlocal boundary layer vertical diffusion in a medium-range forecast model, Mon. Weather Rev., 124, 2322–2339, https://doi.org/10.1175/1520-0493(1996)124<2322:NBLVDI>2.0.CO;2, 1996.

IPCC: Climate change 2013: The physical science basis. In T. F. Stocker et al. (Eds.), Contribution of Working Group I to the Fifth Assessment Report of the Intergovernmental Panel on Climate Change (1535 pp.). Cambridge, UK: Cambridge University Press. https://doi.org/10.1017/CBO9781107415324, 2013.

Ge, G., Gao, J., and Xue, M.: Impacts of Assimilating Measurements of Different State Variables with a Simulated Supercell Storm and Three Dimensional Variational Method, Mon. Weather. Rev., 141 (8), 2759-2777, https://doi.org/10.1175/MWR-D-12-00192.1, 2013.

Giorgi, F., and Mearns, L. O.: Introduction to special section: Regional climate modeling revisited, J. Geophys. Res.-Atmos., 104(D6), 6335-6352, https://doi.org/10.1029/98JD 02072, 1999.

Kalnay, E., Kanamitsu, M., Kistler, R., Collins, W., Deaven, D., Gandin, L., Iredell, M., Saha, S., White, G., Woollen, J., Zhu, Y., Chelliah, M., Ebisuzaki, W., Higgins, W., Janowiak, J., Mo, K. C., Ropelewski, C., Wang, J., Leetmaa, A., Reynolds, R., Jenne, R., and Joseph D.: The NCEP/NCAR 40-year reanalysis project, B. Am. Meteorol. Soc., 77, 437-471, https://doi.org/10.1175/1520-0477(1996)077<0437:TNYRP>2.0.CO;2, 1996.

Kasahara, A., Balgovind, R. C., and Katz, B.: Use of satellite radiometric imagery data for improvement in the analysis of divergent wind in the tropics, Mon. Weather Rev.,116(4), 866-883, https://doi.org/10.1175/1520-0493(1988)116<0866:UOSRID>2.0.CO;2, 1988.

Kasahara, A., Mizzi, A. P., and Donner, L. J.: Impact of Cumulus Initialization on the Spinup of Precipitation Forecasts in the Tropics, Mon. Weather Rev., 120, 1360–1380, https://doi.org/10.1175/1520-0493(1992)120<1360:IOCIOT>2.0.CO;2, 1992.

Khatiwala, S., Visbeck, M., and Cane, M. A.: Accelerated simulation of passive tracers in ocean circulation models, Ocean Model., 9, 51-69, https://doi.org/10.1016/j.ocemod.2004.04.002, 2005.

Kleczek, M. A., Steeneveld, G. J., and Holtslag A. A. M.: Evaluation of the Weather Research and Forecasting Mesoscale Model for GABLS3: Impact of Boundary-Layer Schemes, Boundary Conditions and Spin-Up, Bound.-Lay. Meteorol., 152, 213-243. 10.1007/s10546-014-9925-3., 2014.

Knoll, D. A., and Keyes, D. E.: Jacobian-free Newton-Krylov methods: a survey of approaches and applications, J. Comput. Phys., 193, 357-397, https://doi.org/10.1016/j.jcp.2003.08.010, 2004.

Li, J., Chen, B., Huang, W., and Zhang X.: Investigation of the impact of cloud initialization on numerical prediction of a convective system [in Chinese], J. Trop. Meteorol., 34(2), 198-208, 2018.

Li, Y., Liu, J., Dong, P., and Liu, H.: Analysis of the impact radar data assimilation on the numerical forecast of Jianghuai Rainstorm by using GRAPES-3Dvar [in Chinese], Meteorol. Mon., 37(4), 403-411, 2011.

Linus, M., and Erland, K.: Factors influencing skill improvements in the ECMWF forecasting system, Mon. Weather Rev., 141, 3142-3153, https://doi.org/10.1175/MWR-D-12-00318.1, 2013.

Liu, K., Chen, Q., and Sun, J.: Modification of cumulus convection and planetary boundary layer schemes in the GRAPES global model, J. Meteorol. Res., 29(5), 806-822, 2015.

Liu, S., Jiang, H., Hu, F., Zhang, C., Liu, H., Liang, F., Xin, G., and Wang, J.: Research of spin-up processes of land surface model of RAMs for different initial soil parameters [in Chinese], Acta Meteorol. Sin., 66(3), 351-358, 2008.

Lo, J. C.-F., Yang, Z., and Sr, R. A. P.: Assessment of three dynamical climate downscaling methods using the Weather Research and Forecasting (WRF) model, J. Geophys. Res.-Atmos., 113, D09112, https://doi.org/10.1029/2007JD009216, 2008.

Ma, Z., Liu, Q., Zhao, C., Shen, X., Wang, Y., Jiang, J. H., Li, Z., and Yung, Y.: Application and evaluation of an explicit prognostic cloud cover scheme in GRAPES global forecast system, J. Adv. Model. Earth Syst., 10(3), 652-667, https://doi.org/10.1002/2017MS001234, 2018.

Morcrette, J.-J., Barker, H. W., Cole, J. N. S., Iacono, M. J., and Pincus, R.: Impact of a new radiation package, McRad, in the ECMWF Integrated Forecast System, Mon. Weather Rev., 136, 4773–4798, https://doi.org/10.1175/2008MWR2363.1, 2008.

Pan, H., and Wu, W.: Implementing a mass flux convective parameterization package for the NMC medium-range forecast model (series: Office Note (National Centers for Environmental Prediction) 409, pp. 1–40). Washington, DC: NMC., 1995. Download from https://repository.library.noaa.gov/view/noaa/11429.

Pincus, R., Barker, H. W., and Morcrette, J.-J.: A fast, flexible, approximate technique for computing radiative transfer in inhomogeneous cloud fields, J. Geophys. Res.-Atmos., 108(D13), 4376, https://doi.org/10.1029/2002JD003322, 2003.

Qian, J. H., Seth, A., and Zebiak S.: Reinitialized versus Continuous Simulation for Regional Climate Downscaling, Mon. Weather Rev., 131, 2857-2874, https://doi.org/10.1175/1520-0493(2003)131<2857:RVCSFR>2.0.CO;2, 2003.

Rimac A., Geffen, S. van, and Oerlemans, J.: Numerical simulations of glacier evolution performed using flow-line models of varying complexity, Geosci. Model Dev. Discuss., 1-26. doi:10.5194/gmd-2017-67, 2017.

Scher, S. and Messori, G.: Weather and climate forecasting with neural networks: using general circulation models (GCMs) with different complexity as a study ground, Geosci. Model Dev., 12, 2797-2809. https://doi.org/10.5195/gmd-2019-53, 2019.

Séférian, R., Gehlen, M., Bopp, L., Resplandy, L., Orr, J. C., Marti, O., Dunne, P. J., Christian, J. R., Doney, S. C., IIyina, T., Lindsay, K., Halloran, P. R., Heinze, C., Segschneider, J., Tjiputra, J., Aumont, O., and Romanou, A.: Inconsistent strategies to spin up models in CMIP5: implications for ocean biogeochemical model performance assessment, Geosci. Model Dev., 9, 1827-1851, doi:10.5194/gmd-9-1827-2916, 2016.

Senatore, A., Mendicino, G., Gochis, D. J., Yu, W., Yates, D. N., and Kunstmann, H.: Fully coupled atmosphere-hydrology simulations for the central Mediterranean: Impact of enhanced hydrological parameterization for short and long time scales, J. Adv. Model. Earth Syst., 7, 1693–1715. https://doi.org/10.1002/2015MS000510, 2015.

Shen, X., Su, Y., Hu, J., Wang, J., Sun, J., Xue, J., Han, W., Zhang, H., Lu, H., Zhang, H., Chen, Q., Liu, Y., Liu., Q., Ma, Z., Jin, Z., Li, X., Liu, K., Zhao., B., Zhou, B., Gong., J., Chen, D., and Wang, J: Development and Operation Transformation of GRAPES Global Middle-range Forecast System [in Chinese], J. Appl. Meteorol. Sci., 28(1), 1-10, 2017.

Sheng, C., Pu, Y., and Gao, S.: Effect of Chinese Doppler radar data on nowcasting output of mesoscale model [in Chinese], Chin. J. Atmos. Sci., 30(1), 93-107, 2006.

Souto, M. J., Balseiro, C. F., and Pérez-Muñuzuri, V., Xue, M., and Brewster, K.: Impact of cloud analysis on numerical weather prediction in the Galician region of Span, J. Appl. Meteorol., 42, 129-140, https://doi.org/10.1175/1520-0450(2003)042<0129:IOCAON> 2.0.CO;2, 2003.

Su, Y., Shen, X., Peng, X., Li, X., Wu, X., Zhang, S., and Chen, X.: Application of PRM Scalar Advection Scheme in GRAPES Global Forecast System [in Chinese], Chin. J. Atmos. Sci., 37(6), 1309-1325. doi:10.3878/j.issn.1006-9895.2013.12164., 2013.

Wehbe, Y., Temimi, M., Weston, M., Chaouch, N., Branch, O., Schwitalla, T., Wulfmever, V., Zhan, X., Liu, J., and Mandous, A. A.: Analysis of an extreme weather event in a hyper-arid region using WRF-Hydro coupling, station, and satellite data, Nat. Hazards Earth Syst. Sci., 19, 1129-1149, https://doi.org/10.5194/nhess-19-1129-2019, 2019.

Weiss, S. J., Pyle, M. E., Janjic, Z., Bright, D. R., Kain, J. S., and DiMego, G. J.: The operational High Resolution Window WRF model runs at NCEP: Advantages of multiple model runs for severe convective weather forecasting. Preprints. 24th Conference on Severe Local Storms, American Meteorological Society, Savannah, GA. CD-ROM P10.8. 2008. Download from https://www.spc.noaa.gov/publications/weiss/wrf-hrw.pdf.

Weygandt, S. S., Shapiro, A., and Droegemeier, K. K. : Retrieval of Model Initial Fields from Single-Doppler Observations of a Supercell Thunderstorm. Part II: Thermdynamic Retrieval and Numerical Prediction, Mon. Weather Rev., 130, 454-476, DOI:10.1175/1520-0493(2002)130<0454:ROMIFF>2.0.CO;2, 2002.

Wolcott, S. W., and Warner, T. T.: A moisture analysis procedure utilizing surface and satellite data, Mon. Weather Rev., 109(9), 1989-1998, https://doi.org/10.1175/1520-0493(1981)109<1989:AMAPUS>2.0.CO;2, 1981.

Xie, S. C., Liu, X. H., Zhao, C. F. and Zhang, Y. Y.: Sensitivity of CAM5 simulated Arctic clouds and radiation to ice nucleation parameterization, J. Climate, 26, 5981–5999. doi: http://dx.doi.org/10.1175/JCLI-D-12-00517.1, 2013.

Xue, M., Wang, D., Gao, J., Brewster, K., and Droegemeier K. K.: The advanced regional prediction system (ARPS), storm-scale numerical weather prediction and data assimilation, Meteorol. Atmos. Phys., 82, 139-170, Doi:10.1007/s00703-001-0595-6, 2003.

Xue, C., Chen, X., Wu, Y., Xu, X., and Gao, Y.: Application of radar assimilation in local severe convective weather forecast [in Chinese], Chin. J. Atmos. Sci., 41(4), 673-690, 2017.

Zhang, L., Liu, Y., Liu, Y., Gong, J., Lu, H., Jin, Z., Tian, W., Liu, G., Zhou, B, and Zhao, B.: The operational global four-dimensional variational data assimilation system at the China Meteorological Administration, Q. J. Roy. Meteor. Soc., 145, 1882-1896, https://doi.org/10.1002/qj.3533, 2019.

Zhao, C. F., Klein, S. A., Xie, S. C., Liu, X. H., Boyle, J. S. and Zhang Y.Y.: Aerosol First Indirect effects on non-precipitating low-level liquid cloud properties as simulated by CAM5 at ARM sites, Geophys. Res. Lett., 39, L08806. doi:10.1029/2012GL051213, 2012.

Zhi, X. F., Gao, J., and Zhang, X. L.: An application of the Doppler radar data in the nowcasting using mesoscale model [in Chinese], Scientia. Meteorologica. Sinica., 30(2), 143-150, 2010.

Zhong, Z., Hu, Y. J., Min, J. Z., and Xu, H. L.: Numerical experiments on the spin-up time for seasonal-scale regional climate modeling, Acta Meteorol. Sin., 21(4), 409-419, 2008.

Zhu, L. J., Gong, J. D., Huang, L. P., Chen, D. H., Jiang, Y., and Deng, L. T.: Three-dimensional cloud initial field created and applied to GRAPES numerical weather prediction nowcasting [in Chinese], J. Appl. Meteorol. Sci., 28(1), 38-51, 2017.

Figures

Tables

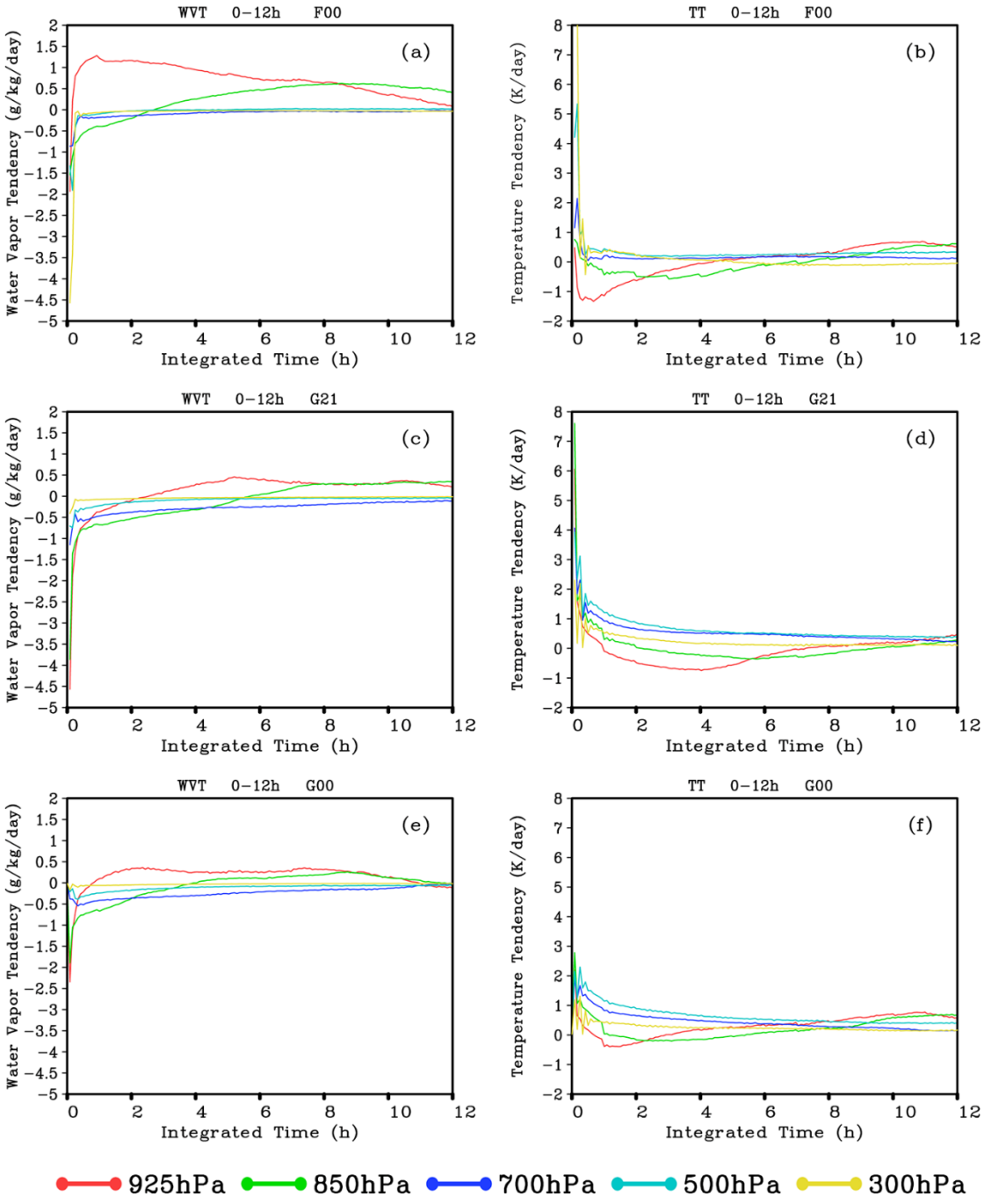

Figure 1. Time evolution of global mean of the total water vapor tendency (WVT) and total temperature tendency (TT) at different vertical levels from 0 to 12h simulated by F00 (a,b), G21(c,d) and G00(e,f) experiments. The unit of WVT and TT is g/kg/day and K/day, respectively.

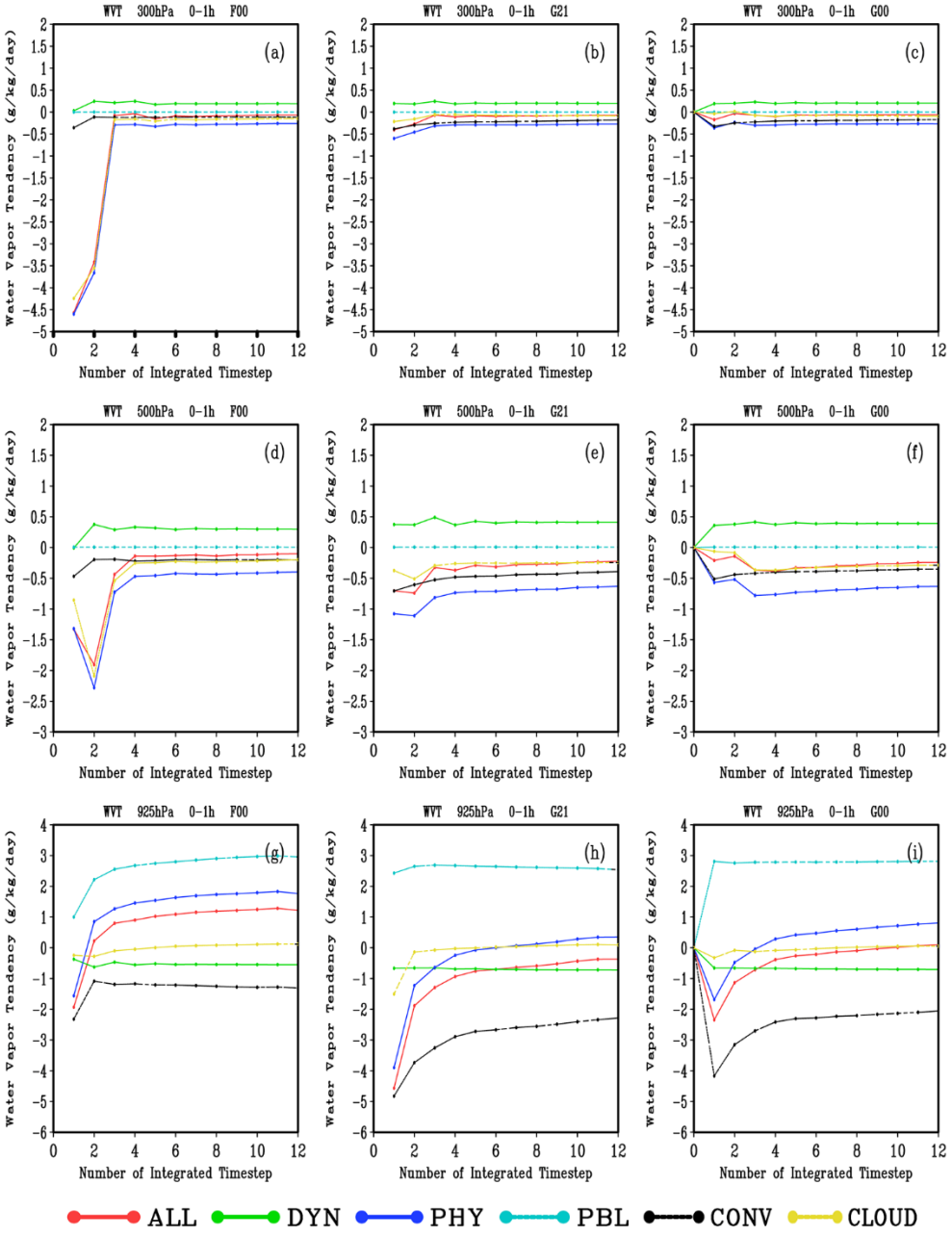

Figure 2. Time evolution of mean water vapor tendency (WVT) of ~~the~~ dynamical core (DYN), ~~and each physical processes~~ planetary boundary layer process (PBL), cumulus convection process (CONV), cloud physical process (CLOUD), the total of all physical processes (PHY, PHY=PBL+CONV+CLOUD) and the total of the model (ALL, ALL=DYN+PHY) at 300hPa, 500hPa and 925hPa heights from 0 to 1h simulated by F00 (a,d,g), G21(b,e,h) and G00(c,f,i) experiments. Unit: g/kg/day.

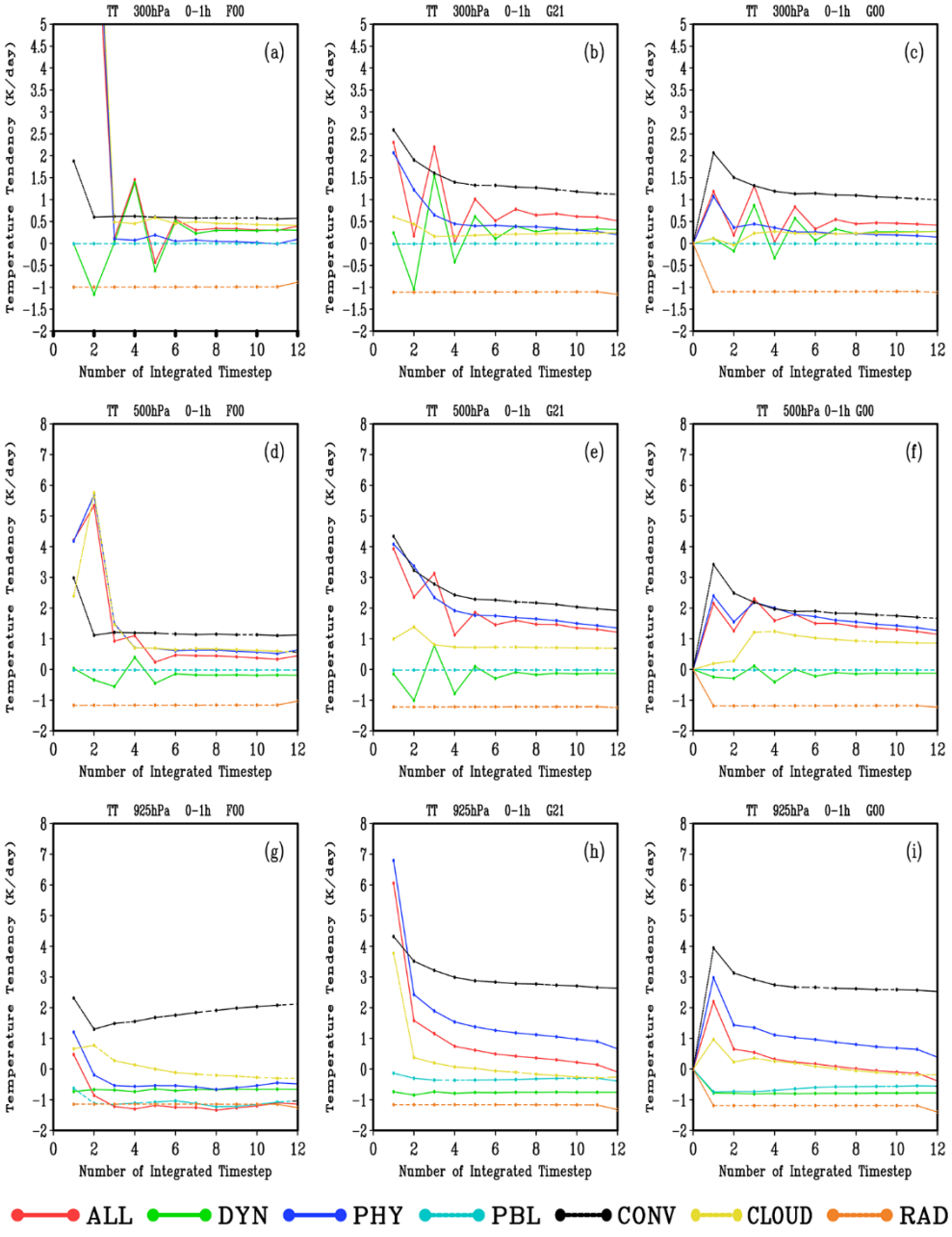

Figure 3. Time evolution of mean temperature tendency (TT) of dynamical core (DYN), radiation process (RAD), planetary boundary layer process (PBL), cumulus convection process (CONV), cloud physical process (CLOUD), the total of all physical processes (PHY, PHY=RAD+PBL+CONV+CLOUD) and the total of the model (ALL, ALL=DYN+PHY) at 300hPa, 500hPa and 925hPa heights from 0 to 1h simulated by F00 (a,d,g), G21(b,e,h) and G00(c,f,i) experiments. Unit: K/day.

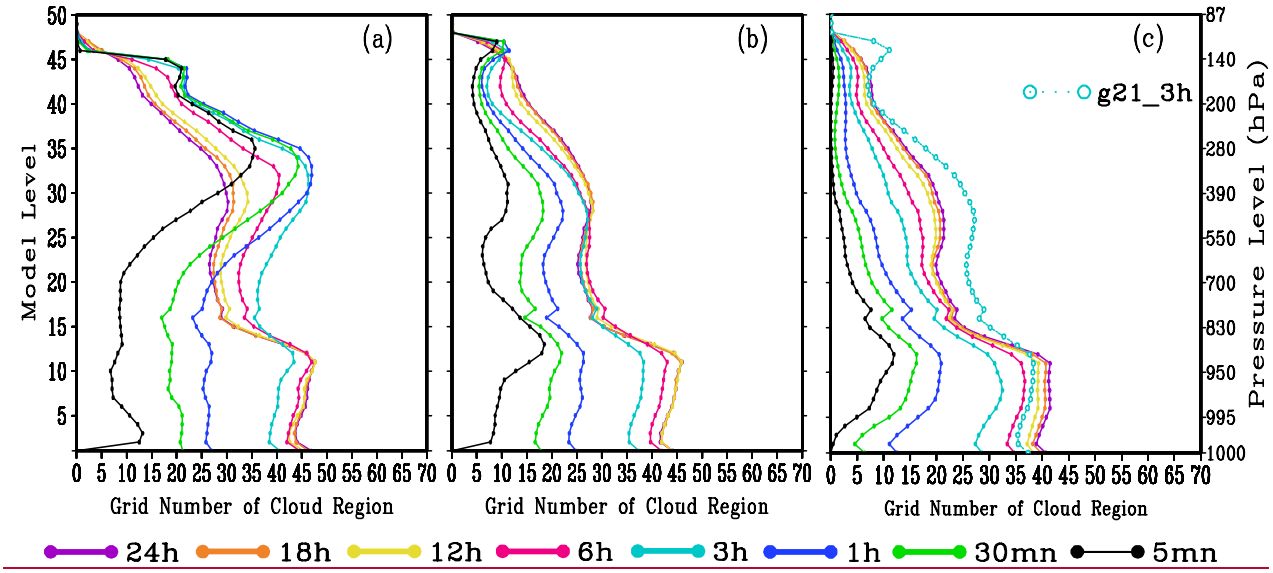

Figure 4. Vertical distribution of the total grid number of cloud （TGNC） at different forecast time simulated by F00 (a), G21(b) and G00(c) experiment, respectively. Unit: number*10000.

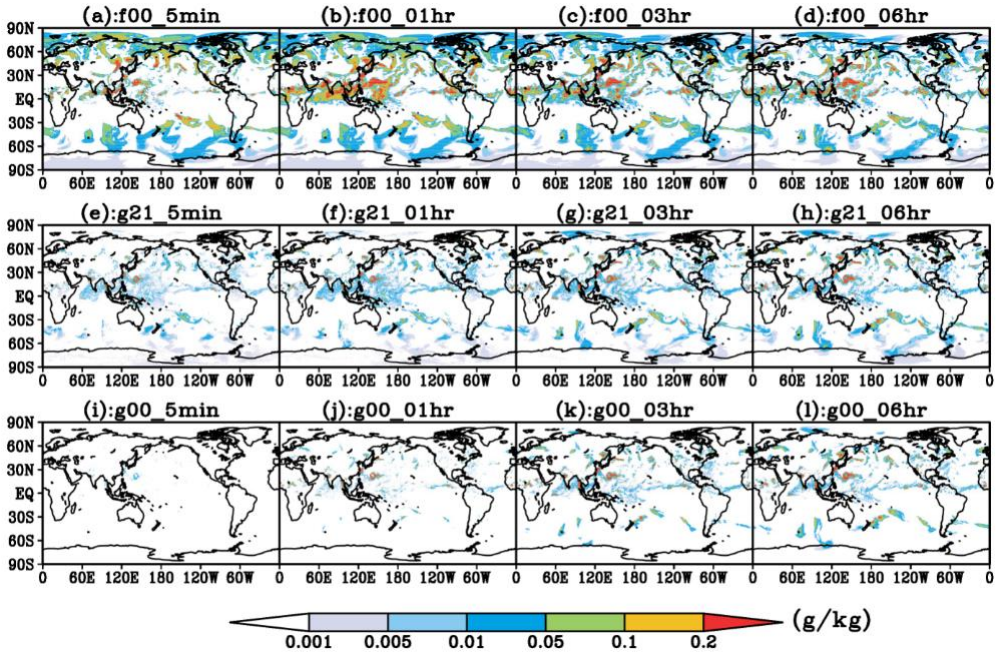

Figure 5. Distributions of all hydrometeor content at 400hPa at different forecast time (5min, 1h, 3h, 6h) simulated by F00 (a-d), G21(e-h) and G00(i-l) experiments, respectively. Unit: g/kg.

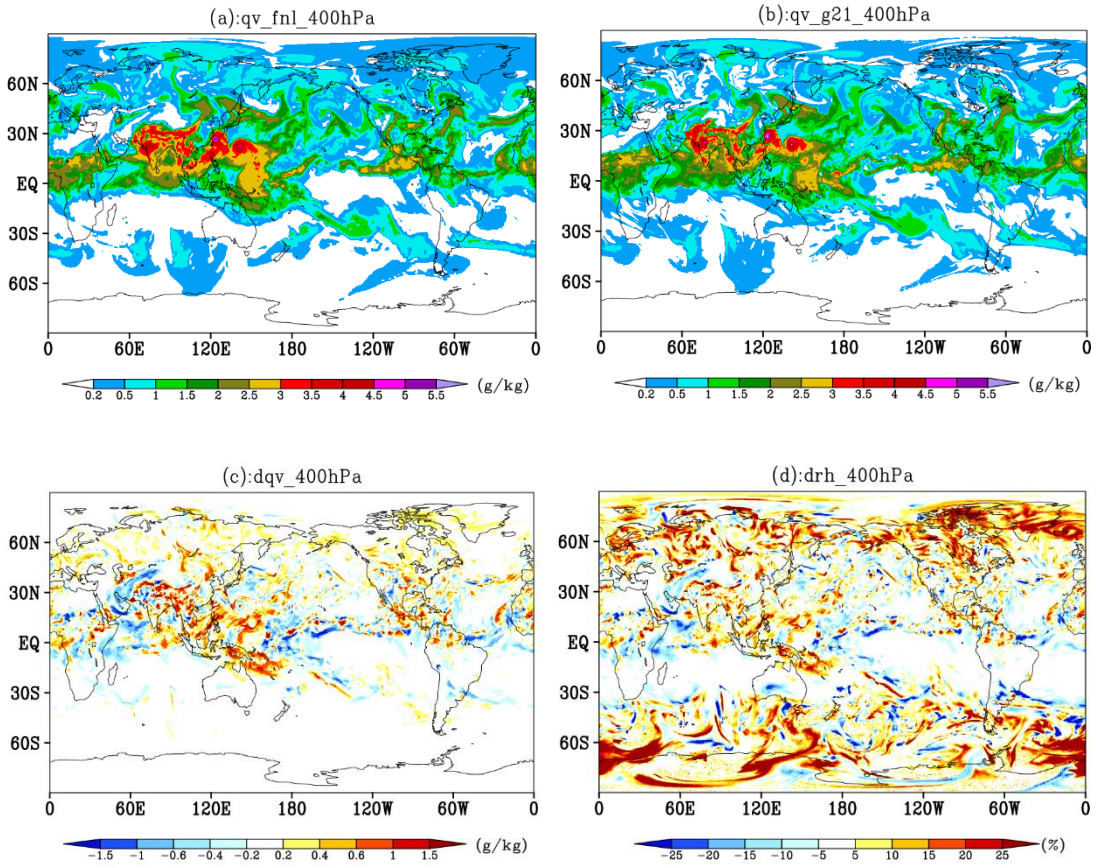

Figure 6. Distribution of water vaper content (WVC) (a-b) simulated by F00 and G21, and the differences of WVC (c) and relative humidity (RH) (d) between F00 and G21 (F00-G21) at 400hPa in their initial fields. The units of WVC and RH are g/kg and %, respectively.

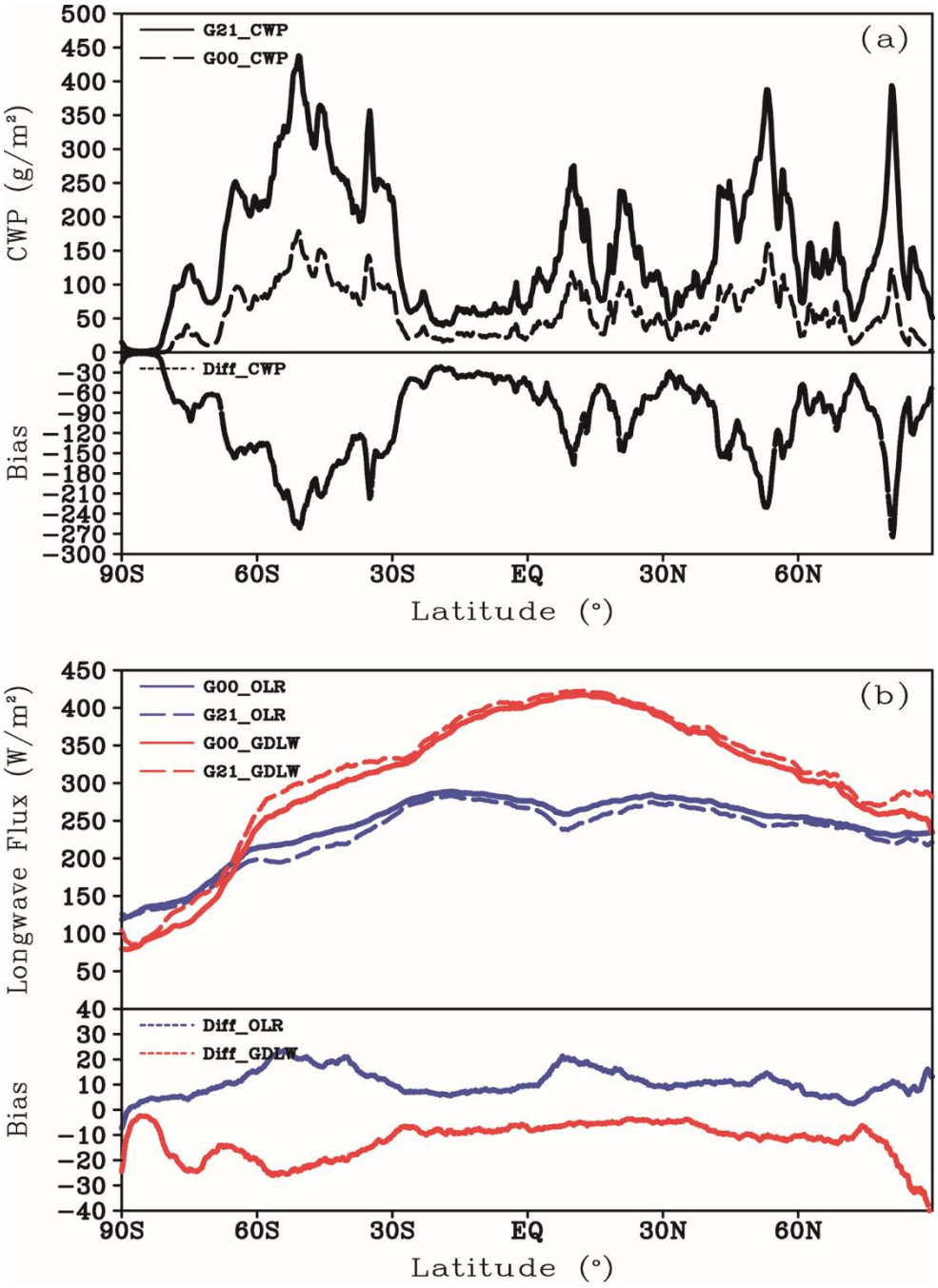

Figure 7. Zonal means and their differences of (a) 3h-averaged cloud water path (CWP), and (b) the outgoing longwave (OLR) at the top of atmosphere and the downward longwave at ground (GDLW) simulated by G21 and G00 experiments for 00~03UTC, August 9, 2019. The units of CWP and OLR/GDLW are g/m^2 and W/m^2, respectively.

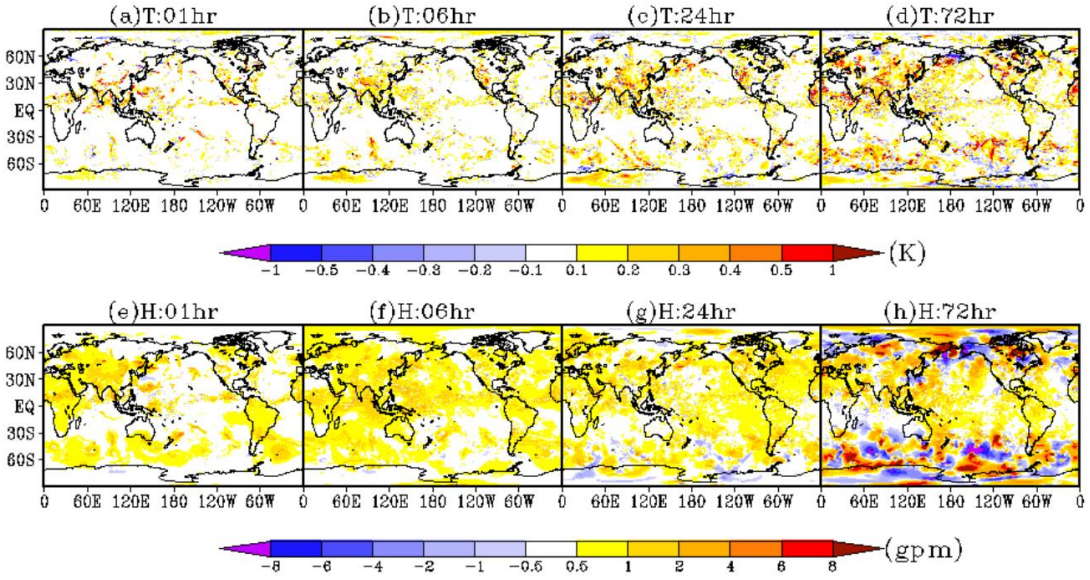

695 **Figure 8. Distribution of the differences (G00 minus G21) of temperature field (a-d) and geopotential height field (e-h) at 500hPa simulated by G00 and G21 experiments. The units of temperature and geopotential height are K and gpm, respectively.**

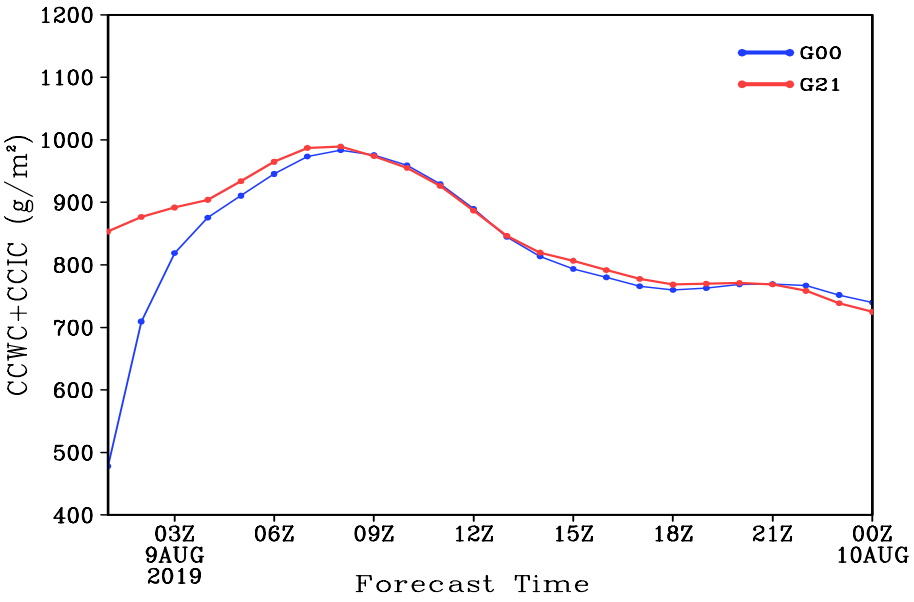

700

Figure 9. Time evolution of the sum of averaged ~~cloud water path~~column cloud water content (CCWC) ~~and ice water path~~column cloud ice content (CCIC) at the typhoon "LEKIMA" region (117°E-130°E，22°N-34°N) simulated by G00 and G21 experiment. Unit: g/m^2.

705

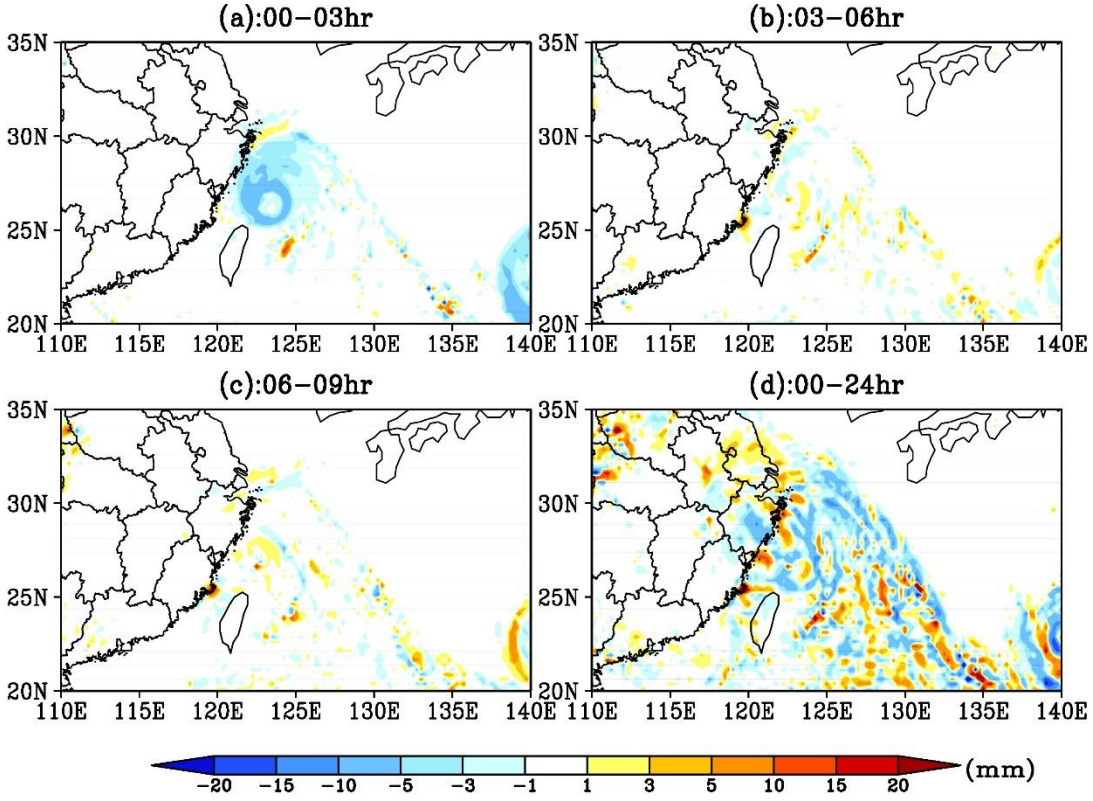

Figure10. Distribution of the differences (G00 minus G21) of 3-hourly and 24h accumulated precipitation (since 00UTC August 8, 2019) of the typhoon "LEKIMA" simulated by G00 and G21 experiments. Unit: mm.

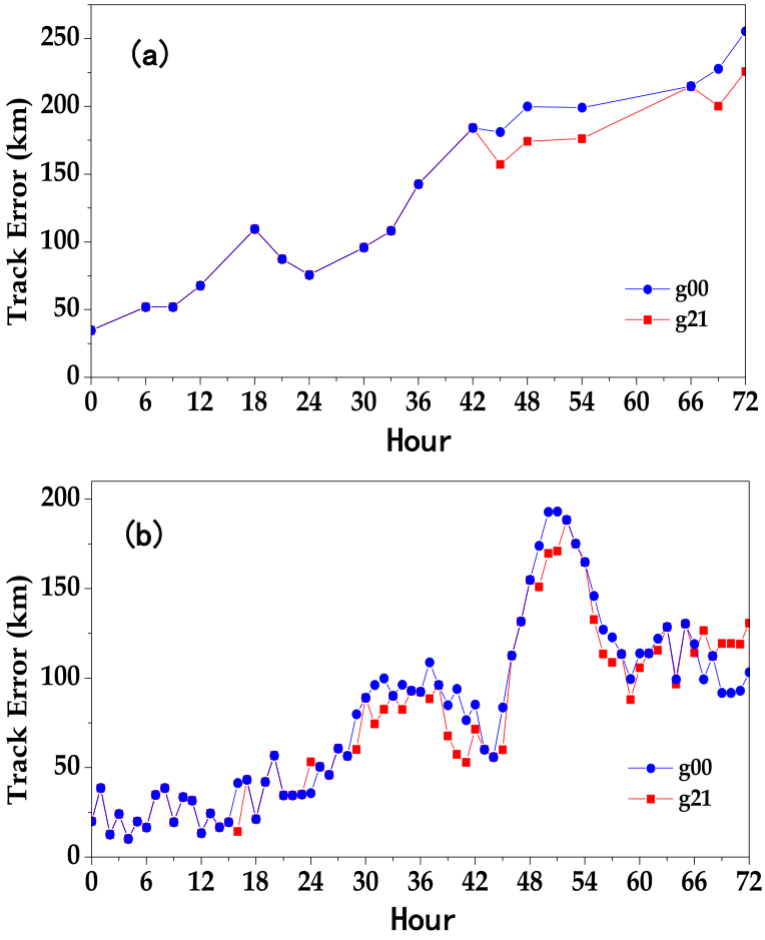

710

Figure 11. Time evolution of the forecasted track errors of G00 and G21 experiments for the typhoon（a） "KROSA" and (b) "LEKIMA" during the forecast period of 72h. Unit: km.

Table 1. Model setup of three experiments used in this study

Experiment Name	Initial Field	Initial Forecast Time	Lead Time (h)
G21	4D-VAR analysis fields	2100 UTC, August 8, 2019	75
G00	4D-VAR analysis fields plus 3-hour integration	0000 UTC, August 9, 2019	72
F00	FNL reanalysis data	0000 UTC, August 9, 2019	72

715